SUPPLEMENTARY MATERIAL

S1. ANISOTROPY INDICES

The anisotropy indices[1,2], apparent diffusion coefficient, axial diffusivity, radial diffusivity, fractional anisotropy and relative anisotropy are defined using the eigenvalues ($\lambda_1 \geq \lambda_2 \geq \lambda_3$) of the diffusion tensor respectively as:

$$ADC = \frac{\lambda_1 + \lambda_2 + \lambda_3}{3} \tag{1}$$

$$AxD = \lambda_1 \tag{2}$$

$$RaD = \frac{\lambda_2 + \lambda_3}{2} \tag{3}$$

$$FA = \frac{\sqrt{(\lambda_1 - \lambda_2)^2 + (\lambda_2 - \lambda_3)^2 + (\lambda_1 - \lambda_3)^2}}{\sqrt{2(\lambda_1^2 + \lambda_2^2 + \lambda_3^2)}} \tag{4}$$

$$RA = \frac{\sqrt{3[(\lambda_1 - \lambda_2)^2 + (\lambda_2 - \lambda_3)^2 + (\lambda_1 - \lambda_3)^2]}}{\lambda_1 + \lambda_2 + \lambda_3}\ . \tag{5}$$

S2. POWER AND SAMPLE SIZE ANALYSIS

S2.1 METHODOLOGY

In this study, non-parametric statistical tests were utilized in the analysis. Therefore, for the power and sample size analysis power and sample size formulations were used for the parametric equivalents of the tests used herein.

Specifically, for each diffusion parameter, statistically significant differences among IDH–TERT subgroups were first identified by Kruskal–Wallis test. For the diffusion parameters with statistical significance, Dunn–Sidak multiple comparisons analysis was performed.

The power analysis procedure of ANOVA was used for Kruskal–Wallis test. For ANOVA power calculations, the numerator (v_n) and denominator (v_d) degrees of freedom and noncentrality parameter[3,4] (ϕ) were calculated as follows:

$$v_n = k - 1\,, \tag{1}$$

$$v_d = k(n-1), \tag{2}$$

$$\phi = \sqrt{\frac{n\Sigma(\mu_i - \mu)^2}{k\sigma^2}}, \tag{3}$$

where *k* is the number of groups compared, *n* is the size of the dataset, σ^2 is the variance of the entire dataset, μ and μ_i are the means of the entire dataset and each of the subgroups, respectively. For determining the statistical power, the power charts corresponding to the aforementioned parameters were consulted[3,4] assuming α=0.05. For α=0.05, power charts were defined for $\phi \geq 1$. The non-centrality parameter of WB–NAWM ADC, λ_1, RaD, λ_2, λ_3 were all less than 1. Consequently, power for these parameters couldn't be determined.

For Dunn–Sidak multiple comparisons analysis and Mann–Whitney test, power and sample size formulations of the two–sided t-test were used[5]. Power was calculated as:

$$Power = \phi(A) = \phi\left[-z_{1-\alpha/2} + \frac{\Delta}{\sqrt{\frac{\sigma_1^2}{n_1} + \frac{\sigma_2^2}{n_2}}}\right], \tag{4}$$

$$\Delta = |\mu_2 - \mu_1|, \tag{5}$$

where A is the are under the standard normal distribution where $\phi(A) = Pr(X \leq A)$, n_i, σ_i and μ_i are the number of samples, standard deviation and mean of the compared groups, respectively, and lastly α is the significance threshold (Type I error).

Sample sizes were estimated as:

$$n_1 = \frac{\left(\frac{\sigma_1^2 + \sigma_2^2}{k}\right) + \left(z_{1-\alpha/2} + z_{1-\beta}\right)^2}{\Delta^2}, \tag{6}$$

$$n_2 = \frac{(k\sigma_1^2 + \sigma_2^2) + \left(z_{1-\alpha/2} + z_{1-\beta}\right)^2}{\Delta^2}, \tag{7}$$

$$k = \frac{n_2}{n_1}, \tag{8}$$

where Δ is defined as Eq. 5, n_i, σ_i and μ_i are the number of samples, standard deviation and mean of the compared groups, respectively, α is the Type I error threshold and β is the Type II error threshold. k in Eq. 8 was calculated with the group sizes in this study. All sample size calculations assumed (α=0.05, 1−β=0.8).

S2.2 RESULTS SUMMARY

In IDH mutation, tests resulting in statistically significant outcomes had power>0.8, and tests resulting in statistically not significant outcomes had power<0.8. However, for TERT mutation, HMeD FA and RA had power=~0.6 even though test were significant with p<0.05. In IDH-TERT subgroup comparisons, although power of ANOVA is poor at 0.4, both WB and HMeD FA and RA had power>0.8 in detecting differences between IDHonly vs. TERTonly and TERTonly vs. DP. WB RaD had power=0.67 despite detecting statistically significant differences between IDHonly and TERTonly subgroups. In summary, the tests had enough statistical power to detect differences between various IDH-TERT based mutation status with few exceptions.

S2.3 TABLES

IDH–TERT Subgroups

Table S1 Power estimates for Kruskal-Wallis and Dunn-Sidak multiple comparisons test performed among IDH–TERT subgroups

IDH-TERT Subgroups Kruskal-Wallis Test Power	**ADC**	**λ_1 (AxD)**	**RaD**	**λ_2**	**λ_3**	**FA**	**RA**
WB–NAWM	-	-	-	-	-	0.40	0.40
HMeD	0.35	0.40	0.40	0.40	0.35	0.40	0.40
IDH–TERT Subgroups Multiple Comparisons Power							
WB–NAWM							
DN vs. IDHonly	0.22	0.72	0.61	0.50	0.66	0.88	0.88
DN vs. TERTonly	0.22	0.72	0.61	0.50	0.66	0.88	0.88
DN vs. DP	0.22	0.72	0.61	0.50	0.66	0.88	0.88
IDHonly vs. TERTonly	0.22	0.72	0.61	0.50	0.66	0.88	0.88
IDHonly vs. DP	0.22	0.72	0.61	0.50	0.66	0.88	0.88
TERTonly vs. DP	0.22	0.72	0.61	0.50	0.66	0.88	0.88
HMeD							
DN vs. IDHonly	0.14	0.30	0.67	0.52	0.77	0.97	0.95
DN vs. TERTonly	0.14	0.30	0.67	0.52	0.77	0.97	0.95
DN vs. DP	0.14	0.30	0.67	0.52	0.77	0.97	0.95
IDHonly vs. TERTonly	0.14	0.30	0.67	0.52	0.77	0.97	0.95
IDHonly vs. DP	0.14	0.30	0.67	0.52	0.77	0.97	0.95
TERTonly vs. DP	0.14	0.30	0.67	0.52	0.77	0.97	0.95

Table S2 Estimated sample size for Group 1 of Dunn–Sidak multiple comparisons tests. Sample size estimates assume (α=0.05, 1–β=0.8).

IDH–TERT Subgroups Multiple Comparisons Group 1 Estimated Sample Size							
	ADC	**λ_1 (AxD)**	**RaD**	**λ_2**	**λ_3**	**FA**	**RA**
WB–NAWM							
DN vs. IDHonly	117	26	34	43	30	18	17
DN vs. TERTonly	117	26	34	43	30	18	17
DN vs. DP	117	26	34	43	30	18	17
IDHonly vs. TERTonly	117	26	34	43	30	18	17
IDHonly vs. DP	117	26	34	43	30	18	17
TERTonly vs. DP	117	26	34	43	30	18	17
HMeD							
DN vs. IDHonly	228	80	31	43	24	13	14
DN vs. TERTonly	228	80	31	43	24	13	14
DN vs. DP	228	80	31	43	24	13	14
IDHonly vs. TERTonly	228	80	31	43	24	13	14
IDHonly vs. DP	228	80	31	43	24	13	14
TERTonly vs. DP	228	80	31	43	24	13	14

Table S3 Estimated sample size for Group 2 of Dunn–Sidak multiple comparisons tests. Sample size estimates assume (α=0.05, 1–β=0.8).

IDH–TERT Subgroups Multiple Comparisons Group 2 Estimated Sample Size							
	ADC	**λ_1 (AxD)**	**RaD**	**λ_2**	**λ_3**	**FA**	**RA**
WB–NAWM							
DN vs. IDHonly	95	21	27	35	24	14	14
DN vs. TERTonly	95	21	27	35	24	14	14
DN vs. DP	95	21	27	35	24	14	14
IDHonly vs. TERTonly	95	21	27	35	24	14	14
IDHonly vs. DP	95	21	27	35	24	14	14
TERTonly vs. DP	95	21	27	35	24	14	14
HMeD							
DN vs. IDHonly	181	64	24	34	19	10	11
DN vs. TERTonly	181	64	24	34	19	10	11
DN vs. DP	181	64	24	34	19	10	11
IDHonly vs. TERTonly	181	64	24	34	19	10	11
IDHonly vs. DP	181	64	24	34	19	10	11
TERTonly vs. DP	181	64	24	34	19	10	11

IDH and TERT Mutation Status

Table S4 Power estimates for Mann–Whitney test performed between IDH and TERT mutation status. Sample size estimates assume (α=0.05, 1−β=0.8).

	ADC	λ_1 (AxD)	RaD	λ_2	λ_3	FA	RA
IDH Mutation Mann-Whitney Test Power							
WB–NAWM							
Power	0.50	0.92	0.91	0.88	0.92	0.99	0.99
Estimated WT Sample Size	52	18	18	21	18	11	11
Estimated MUT Sample Size	85	29	30	34	29	18	18
HMeD							
Power	0.10	0.91	0.18	0.07	0.35	0.92	0.90
Estimated WT Sample Size	408	17	168	883	73	16	17
Estimated MUT Sample Size	714	30	300	1569	130	29	31
TERT Mutation Mann-Whitney Test Power							
WB–NAWM							
Power	0.32	0.14	0.46	0.53	0.39	0.47	0.46
Estimated WT Sample Size	113	305	71	60	87	70	72
Estimated MUT Sample Size	133	358	84	71	102	82	85
HMeD							
Power	0.12	0.10	0.35	0.23	0.45	0.66	0.60
Estimated WT Sample Size	411	504	98	162	73	44	51
Estimated MUT Sample Size	489	595	116	193	86	52	60

S3. **INVESTIGATING GENOTYPE PREDICTION BY THRESHOLDING**

S3.1 METHODOLOGY

Using in-house MATLAB® code, each variable's unique values for the patient cohort were determined. Each unique value was used as a decision threshold for each genotype and, true positive (TP), true negative (TN), false positive (FP) and false negative (FN) values were obtained. Receiver operating characteristic[6] (ROC) curve was plotted by computing true positive rate (TPR) and false positive rate (FPR) defined as

$$TPR = \frac{TP}{TP + FN}, \tag{9}$$

$$FPR = \frac{FP}{FP + TN} \tag{10}$$

for each threshold value (see Figure S.1 through Figure S.24). ROC curve's closest point (in the Euclidean norm sense) to the top left corner point, (TPR=0, FPR=1), which corresponds to sensitivity=1 and specificity=1, was chosen as the optimal operating threshold for each case (see Table S6).

For assessing the optimal decision threshold performance, the positive predictive values (PPV) and the negative predictive values (NPV), defined as

$$PPV = \frac{TP}{TP + FP}, \tag{11}$$

$$NPV = \frac{TN}{TN + FN}, \tag{12}$$

were calculated at the optimal operating threshold in each case (see Table S11) using TP, TN, FP and FN values (see Table S7 through Table S10).

Each variable's overall performance for each mutation group was assessed from the corresponding ROC curve's area under the curve[6] (AUC) (see Table S12**Error! Reference source not found.**).

Table S5 Truth and predictions from thresholding

Value >= Threshold	**Truth**	**Value <= Threshold**
lTP	**P**	uFN
lFP	**N**	uTN
Threshold		
lFN	**P**	uTP
lTN	**N**	uFP

Each threshold was used once as a lower bound (Value >= Threshold), once as an upper bound (Value <= Threshold) as the decision criterion and all of the aforementioned steps were realized. Table S5 presents theoretical characterization of TP, FP, TN and FN values for each decision criterion, where P and N denote (ground truth) number of positives and negatives respectively, lTP and uTP denote TP values from the lower and upper bound criterion respectively (likewise for FP, TN, FN). By Table S5,

$$lTP = uFN, \qquad lFP = uTN, \qquad lFN = uTP \quad and \qquad lTN = uFP, \tag{13}$$

which implies after rudimentary derivations using Eq.(9) and Eq.(10) that

$$lTPR = 1 - uTPR \quad and \quad lFPR = 1 - uFPR\,, \tag{14}$$

where lTPR and uTPR denote TPR values from the lower and upper bound criteria respectively (likewise for FPR).

Equation (14) implies that AUCs from lower bound thresholding (LBTh) and upper bound thresholding (UBTH) for the same variable are related as

$$lAUC = 1 - uAUC \tag{15}$$

where lAUC and uAUC are the AUCs for LBTH and UBTh respectively (compare Figure S.1 through Figure S.12 with Figure S.13 through Figure S.24). Table S12 shows the complementary nature of the AUC

values for the two types of decision criteria by using complementary color coding of the table cells for LBTh and UBTh sections resulting in the same cell color pattern for both sections.

AUC is considered as a measure of classifier performance[6] by its proximity to 1. Accordingly, if for a given threshold a decision criterion results in low AUC value, the complementary decision criterion will result in a higher performance by Eq. (14), e.g., compare whole brain RA UBTh for IDHmut versus LBTh in Table S12. By contrast, an AUC value close to 0.5 indicates a poor classifier performance for the variable under investigation.

S3.2 TABLES

Table S6 Optimal operating thresholds from the ROC curves for lower and upper bound thresholding criteria

WholeBrain Thresholds for Optimal Operating Point (Value>=Threshold)								**LobeDifference Thresholds for Optimal Operating Point (Value>=Threshold)**							
	ADC	**AxD**	**RaD**	**λ_2**	**λ_3**	**FA**	**RA**		**ADC**	**AxD**	**RaD**	**λ_2**	**λ_3**	**FA**	**RA**
IDHmut	795.7761	1146.3266	610.8608	719.3448	452.3129	0.4119	0.6230	**IDHmut**	-14.5305	2.5934	-10.6669	-15.7392	-9.4922	-0.0121	-0.0212
TERTmut	774.7806	1130.2279	601.8153	710.4823	471.3025	0.4193	0.6557	**TERTmut**	-5.8207	-10.8992	-5.2141	-7.4416	-7.3585	0.0093	0.0211
DN	770.3922	1140.0467	590.0661	703.3609	466.8716	0.4115	0.6439	**DN**	-6.4695	-3.9022	-7.1776	-7.4111	-7.5587	0.0073	0.0079
IDHonly	797.8019	1154.1877	591.9729	719.3448	473.8798	0.4119	0.6754	**IDHonly**	-12.1449	-5.5384	-10.0779	-15.7392	-9.4383	0.0033	0.0068
TERTonly	783.9301	1154.5920	607.0352	716.7720	504.5233	0.4395	0.6967	**TERTonly**	-4.9110	-10.8992	-9.2243	-7.4416	-3.4013	0.0093	0.0236
DP	774.7806	1130.2279	573.2614	702.1266	453.5861	0.4199	0.6557	**DP**	-5.8207	2.5934	-5.2141	-3.6308	-6.7945	-0.0021	-0.0001
WholeBrain Thresholds for Optimal Operating Point (Value<=Threshold)								**LobeDifference Thresholds for Optimal Operating Point (Value<=Threshold)**							
IDHmut	771.3303	1154.1877	593.1958	707.8263	473.8798	0.4026	0.6424	**IDHmut**	-6.5021	-13.4705	-8.1743	-7.6584	-4.5276	0.0069	0.0115
TERTmut	770.0521	1139.6092	590.6676	704.9942	454.4713	0.4076	0.6356	**TERTmut**	-10.5550	-5.7686	-9.8977	-16.8043	-9.4922	0.0025	0.0064
DN	778.0347	1142.0141	597.6112	716.4839	471.1043	0.4168	0.6585	**DN**	5.3385	-3.0368	-3.6351	0.2885	-1.6366	0.0098	0.0169
IDHonly	773.8802	1128.9947	568.7002	697.7157	457.2504	0.4124	0.6542	**IDHonly**	-6.5021	-11.0708	-8.1743	-7.6584	-8.8492	0.0069	0.0115
TERTonly	794.3401	1138.1576	587.6684	700.0439	452.0436	0.3814	0.5918	**TERTonly**	-14.7161	-5.8403	-10.7551	-17.0226	-10.7523	0.0005	-0.0513
DP	770.0521	1151.7001	592.6136	704.9942	472.4193	0.4395	0.6725	**DP**	-13.1322	-20.7117	-9.8977	-14.8287	-4.5276	0.0030	0.0064

Table S7 Number of true positives (TP) for WB-NAWM and HMeDs at the optimal operating thresholds

WholeBrain TPs for Optimal Operating Point (Value>=Threshold)							
	ADC	**AxD**	**RaD**	**λ_2**	**λ_3**	**FA**	**RA**
IDHmut	9	27	9	11	25	27	31
TERTmut	20	24	20	22	23	14	15
DN	7	5	7	7	7	5	5
IDHonly	6	15	10	7	9	16	12
TERTonly	13	6	14	13	13	3	3
DP	7	15	11	10	11	10	11

LobeDifference TPs for Optimal Operating Point (Value>=Threshold)							
	ADC	**AxD**	**RaD**	**λ_2**	**λ_3**	**FA**	**RA**
IDHmut	26	13	26	28	27	41	41
TERTmut	17	26	13	16	15	21	18
DN	8	7	7	8	6	5	6
IDHonly	12	7	15	17	16	10	10
TERTonly	8	16	7	7	4	17	15
DP	9	8	9	9	10	13	11

WholeBrain TPs for Optimal Operating Point (Value<=Threshold)							
	ADC	**AxD**	**RaD**	**l2**	**l3**	**FA**	**RA**
IDHmut	25	21	29	26	28	13	15
TERTmut	15	21	16	15	12	22	21
DN	6	6	6	7	5	7	7
IDHonly	17	7	13	14	14	10	11
TERTonly	13	14	5	5	4	13	13
DP	10	11	12	10	12	12	10

LobeDifference TPs for Optimal Operating Point (Value<=Threshold)							
	ADC	**AxD**	**RaD**	**l2**	**l3**	**FA**	**RA**
IDHmut	27	23	22	25	24	33	31
TERTmut	19	21	21	17	22	15	16
DN	7	4	6	7	6	7	7
IDHonly	19	17	14	17	12	20	18
TERTonly	10	12	13	11	15	3	1
DP	8	7	8	7	10	13	13

Table S8 Number of false positives (FP) for WB-NAWM and HMeDs at the optimal operating thresholds

WholeBrain FPs for Optimal Operating Point (Value>=Threshold)								**LobeDifference FPs for Optimal Operating Point (Value>=Threshold)**							
	ADC	**AxD**	**RaD**	**λ_2**	**λ_3**	**FA**	**RA**		**ADC**	**AxD**	**RaD**	**λ_2**	**λ_3**	**FA**	**RA**
IDHmut	9	9	13	13	23	8	11	**IDHmut**	18	11	14	17	11	27	27
TERTmut	11	22	9	13	13	15	16	**TERTmut**	12	14	14	15	17	6	4
DN	33	33	32	33	33	31	30	**DN**	22	21	23	22	27	25	30
IDHonly	11	15	27	17	25	19	11	**IDHonly**	27	23	24	28	21	26	27
TERTonly	13	22	11	13	9	16	17	**TERTonly**	17	24	29	24	21	10	4
DP	24	31	34	32	36	18	20	**DP**	20	16	18	16	21	39	37
WholeBrain FPs for Optimal Operating Point (Value<=Threshold)								**LobeDifference FPs for Optimal Operating Point (Value<=Threshold)**							
	ADC	**AxD**	**RaD**	**l2**	**l3**	**FA**	**RA**		**ADC**	**AxD**	**RaD**	**l2**	**l3**	**FA**	**RA**
IDHmut	8	20	9	8	9	18	19	**IDHmut**	13	4	16	14	20	7	7
TERTmut	15	11	17	18	13	12	12	**TERTmut**	14	19	12	7	11	17	17
DN	35	28	34	36	29	33	35	**DN**	49	41	44	46	42	39	40
IDHonly	21	17	9	11	15	27	28	**IDHonly**	21	13	24	22	25	20	20
TERTonly	39	17	25	23	18	6	6	**TERTonly**	16	27	17	12	17	21	0
DP	20	29	24	23	24	39	37	**DP**	23	14	25	20	34	21	20

Table S9 Number of false negatives (FN) for WB-NAWM and HMeDs at the optimal operating thresholds

WholeBrain FNs for Optimal Operating Point (Value>=Threshold)							
	ADC	**AxD**	**RaD**	**λ_2**	**λ_3**	**FA**	**RA**
IDHmut	32	14	32	30	16	14	10
TERTmut	17	13	17	15	14	23	22
DN	2	4	2	2	2	4	4
IDHonly	18	9	14	17	15	8	12
TERTonly	7	14	6	7	7	17	17
DP	10	2	6	7	6	7	6

LobeDifference FNs for Optimal Operating Point (Value>=Threshold)							
	ADC	**AxD**	**RaD**	**λ_2**	**λ_3**	**FA**	**RA**
IDHmut	15	28	15	13	14	0	0
TERTmut	20	11	24	21	22	16	19
DN	1	2	2	1	3	4	3
IDHonly	12	17	9	7	8	14	14
TERTonly	12	4	13	13	16	3	5
DP	8	9	8	8	7	4	6

WholeBrain FNs for Optimal Operating Point (Value<=Threshold)							
	ADC	**AxD**	**RaD**	**l2**	**l3**	**FA**	**RA**
IDHmut	16	20	12	15	13	28	26
TERTmut	22	16	21	22	25	15	16
DN	3	3	3	2	4	2	2
IDHonly	7	17	11	10	10	14	13
TERTonly	7	6	15	15	16	7	7
DP	7	6	5	7	5	5	7

LobeDifference FNs for Optimal Operating Point (Value<=Threshold)							
	ADC	**AxD**	**RaD**	**l2**	**l3**	**FA**	**RA**
IDHmut	14	18	19	16	17	8	10
TERTmut	18	16	16	20	15	22	21
DN	2	5	3	2	3	2	2
IDHonly	5	7	10	7	12	4	6
TERTonly	10	8	7	9	5	17	19
DP	9	10	9	10	7	4	4

Table S10 Number of true negatives (TN) for WB-NAWM and HMeDs at the optimal operating thresholds

WholeBrain TNs for Optimal Operating Point (Value>=Threshold)							
	ADC	**AxD**	**RaD**	**λ_2**	**λ_3**	**FA**	**RA**
IDHmut	20	20	16	16	6	21	18
TERTmut	22	11	24	20	20	18	17
DN	28	28	29	28	28	30	31
IDHonly	35	31	19	29	21	27	35
TERTonly	37	28	39	37	41	34	33
DP	29	22	19	21	17	35	33

LobeDifference TNs for Optimal Operating Point (Value>=Threshold)							
	ADC	**AxD**	**RaD**	**λ_2**	**λ_3**	**FA**	**RA**
IDHmut	11	18	15	12	18	2	2
TERTmut	21	19	19	18	16	27	29
DN	39	40	38	39	34	36	31
IDHonly	19	23	22	18	25	20	19
TERTonly	33	26	21	26	29	40	46
DP	33	37	35	37	32	14	16

WholeBrain TNPs for Optimal Operating Point (Value<=Threshold)							
	ADC	**AxD**	**RaD**	**l2**	**l3**	**FA**	**RA**
IDHmut	21	9	20	21	20	11	10
TERTmut	18	22	16	15	20	21	21
DN	26	33	27	25	32	28	26
IDHonly	25	29	37	35	31	19	18
TERTonly	11	33	25	27	32	44	44
DP	33	24	29	30	29	14	16

LobeDifference TNs for Optimal Operating Point (Value<=Threshold)							
	ADC	**AxD**	**RaD**	**l2**	**l3**	**FA**	**RA**
IDHmut	16	25	13	15	9	22	22
TERTmut	19	14	21	26	22	16	16
DN	12	20	17	15	19	22	21
IDHonly	25	33	22	24	21	26	26
TERTonly	34	23	33	38	33	29	50
DP	30	39	28	33	19	32	33

Table S11 Positive Predictive Values (PPV), Negative Predictive Values (NPV) for variable values obtained from WB-NAWM and HMeDs at the optimal operating thresholds. Cells are color coded by their values within each classification criteria.

WholeBrain PPVs for Optimal Operating Point (Value>=Threshold)							
	ADC	AxD	RaD	λ_2	λ_3	FA	RA
IDHmut	0.5000	0.7500	0.4091	0.4583	0.5208	0.7714	0.7381
TERTmut	0.6452	0.5217	0.6897	0.6286	0.6389	0.4828	0.4839
DN	0.1750	0.1316	0.1795	0.1750	0.1750	0.1389	0.1429
IDHonly	0.3529	0.5000	0.2703	0.2917	0.2647	0.4571	0.5217
TERTonly	0.5000	0.2143	0.5600	0.5000	0.5909	0.1579	0.1500
DP	0.2258	0.3261	0.2444	0.2381	0.2340	0.3571	0.3548

LobeDifference PPVs for Optimal Operating Point (Value>=Threshold)							
	ADC	AxD	RaD	λ_2	λ_3	FA	RA
IDHmut	0.5909	0.5417	0.6500	0.6222	0.7105	0.6029	0.6029
TERTmut	0.5862	0.6500	0.4815	0.5161	0.4688	0.7778	0.8182
DN	0.2667	0.2500	0.2333	0.2667	0.1818	0.1667	0.1667
IDHonly	0.3077	0.2333	0.3846	0.3778	0.4324	0.2778	0.2703
TERTonly	0.3200	0.4000	0.1944	0.2258	0.1600	0.6296	0.7895
DP	0.3103	0.3333	0.3333	0.3600	0.3226	0.2500	0.2292

WholeBrain NPVs for Optimal Operating Point (Value>=Threshold)							
IDHmut	0.3846	0.5882	0.3333	0.3478	0.2727	0.6000	0.6429
TERTmut	0.5641	0.4583	0.5854	0.5714	0.5882	0.4390	0.4359
DN	0.9333	0.8750	0.9355	0.9333	0.9333	0.8824	0.8857
IDHonly	0.6604	0.7750	0.5758	0.6304	0.5833	0.7714	0.7447
TERTonly	0.8409	0.6667	0.8667	0.8409	0.8542	0.6667	0.6600
DP	0.7436	0.9167	0.7600	0.7500	0.7391	0.8333	0.8462

LobeDifference NPVs for Optimal Operating Point (Value>=Threshold)							
IDHmut	0.4231	0.3913	0.5000	0.4800	0.5625	1.0000	1.0000
TERTmut	0.5122	0.6333	0.4419	0.4615	0.4211	0.6279	0.6042
DN	0.9750	0.9524	0.9500	0.9750	0.9189	0.9000	0.9118
IDHonly	0.6129	0.5750	0.7097	0.7200	0.7576	0.5882	0.5758
TERTonly	0.7333	0.8667	0.6176	0.6667	0.6444	0.9302	0.9020
DP	0.8049	0.8043	0.8140	0.8222	0.8205	0.7778	0.7273

WholeBrain PPVs for Optimal Operating Point (Value<=Threshold)							
IDHmut	0.7576	0.5122	0.7632	0.7647	0.7568	0.4194	0.4412
TERTmut	0.5000	0.6563	0.4848	0.4545	0.4800	0.6471	0.6364
DN	0.1463	0.1765	0.1500	0.1628	0.1471	0.1750	0.1667
IDHonly	0.4474	0.2917	0.5909	0.5600	0.4828	0.2703	0.2821
TERTonly	0.2500	0.4516	0.1667	0.1786	0.1818	0.6842	0.6842
DP	0.3333	0.2750	0.3333	0.3030	0.3333	0.2353	0.2128

LobeDifference PPVs for Optimal Operating Point (Value<=Threshold)							
IDHmut	0.6750	0.8519	0.5789	0.6410	0.5455	0.8250	0.8158
TERTmut	0.5758	0.5250	0.6364	0.7083	0.6667	0.4688	0.4848
DN	0.1250	0.0889	0.1200	0.1321	0.1250	0.1522	0.1489
IDHonly	0.4750	0.5667	0.3684	0.4359	0.3243	0.5000	0.4737
TERTonly	0.3846	0.3077	0.4333	0.4783	0.4688	0.1250	1.0000
DP	0.2581	0.3333	0.2424	0.2593	0.2273	0.3824	0.3939

WholeBrain NPVs for Optimal Operating Point (Value<=Threshold)							
IDHmut	0.5676	0.3103	0.6250	0.5833	0.6061	0.2821	0.2778
TERTmut	0.4500	0.5789	0.4324	0.4054	0.4444	0.5833	0.5676
DN	0.8966	0.9167	0.9000	0.9259	0.8889	0.9333	0.9286
IDHonly	0.7813	0.6304	0.7708	0.7778	0.7561	0.5758	0.5806
TERTonly	0.6111	0.8462	0.6250	0.6429	0.6667	0.8627	0.8627
DP	0.8250	0.8000	0.8529	0.8108	0.8529	0.7368	0.6957

LobeDifference NPVs for Optimal Operating Point (Value<=Threshold)							
IDHmut	0.5333	0.5814	0.4063	0.4839	0.3462	0.7333	0.6875
TERTmut	0.5135	0.4667	0.5676	0.5652	0.5946	0.4211	0.4324
DN	0.8571	0.8000	0.8500	0.8824	0.8636	0.9167	0.9130
IDHonly	0.8333	0.8250	0.6875	0.7742	0.6364	0.8667	0.8125
TERTonly	0.7727	0.7419	0.8250	0.8085	0.8684	0.6304	0.7246
DP	0.7692	0.7959	0.7568	0.7674	0.7308	0.8889	0.8919

Table S12 Area under the curve (AUC) values for ROC curves for WB-NAWM and HMeDs obtained by lower and upper bound thresholding. Cells are color coded by their values within each decision criteria. Complementary color coding was used for lower and upper bound thresholding AUC values.

WholeBrain AUCs for Optimal Operating Point (Value>=Threshold)							
	ADC	**AxD**	**RaD**	**λ_2**	**λ_3**	**FA**	**RA**
IDHmut	0.3322	0.7115	0.2641	0.2717	0.2675	0.7653	0.7653
TERTmut	0.5872	0.4144	0.6200	0.6331	0.6077	0.3718	0.3726
DN	0.5428	0.4117	0.5610	0.5574	0.5556	0.4281	0.4353
IDHonly	0.3822	0.6386	0.3370	0.3243	0.3533	0.6775	0.6730
TERTonly	0.6760	0.2970	0.7470	0.7400	0.7460	0.2240	0.2200
DP	0.4229	0.6093	0.3885	0.4140	0.3729	0.6326	0.6382
WholeBrain AUCs for Optimal Operating Point (Value<=Threshold)							
IDHmut	0.6678	0.2885	0.7359	0.7283	0.7325	0.2347	0.2347
TERTmut	0.4128	0.5856	0.3800	0.3669	0.3923	0.6282	0.6274
DN	0.4572	0.5883	0.4390	0.4426	0.4444	0.5719	0.5647
IDHonly	0.6178	0.3614	0.6630	0.6757	0.6467	0.3225	0.3270
TERTonly	0.3240	0.7030	0.2530	0.2600	0.2540	0.7760	0.7800
DP	0.5771	0.3907	0.6115	0.5860	0.6271	0.3674	0.3618

LobeDifference AUCs for Optimal Operating Point (Value>=Threshold)							
	ADC	**AxD**	**RaD**	**λ_2**	**λ_3**	**FA**	**RA**
IDHmut	0.4500	0.2851	0.5711	0.5248	0.6358	0.2212	0.2170
TERTmut	0.4758	0.5717	0.3964	0.4226	0.3653	0.6732	0.6618
DN	0.7341	0.7377	0.7013	0.7341	0.6448	0.4973	0.5155
IDHonly	0.4103	0.3025	0.5145	0.4692	0.5770	0.3098	0.3134
TERTonly	0.4310	0.6250	0.3050	0.3420	0.2590	0.8330	0.8280
DP	0.5438	0.4584	0.5760	0.5705	0.5849	0.3651	0.3552
LobeDifference AUCs for Optimal Operating Point (Value<=Threshold)							
IDHmut	0.5500	0.7149	0.4289	0.4752	0.3642	0.7788	0.7830
TERTmut	0.5242	0.4283	0.6036	0.5774	0.6347	0.3268	0.3382
DN	0.2659	0.2623	0.2987	0.2659	0.3552	0.5027	0.4845
IDHonly	0.5897	0.6975	0.4855	0.5308	0.4230	0.6902	0.6866
TERTonly	0.5690	0.3750	0.6950	0.6580	0.7410	0.1670	0.1720
DP	0.4562	0.5416	0.4240	0.4295	0.4151	0.6349	0.6448

S3.3 FIGURES

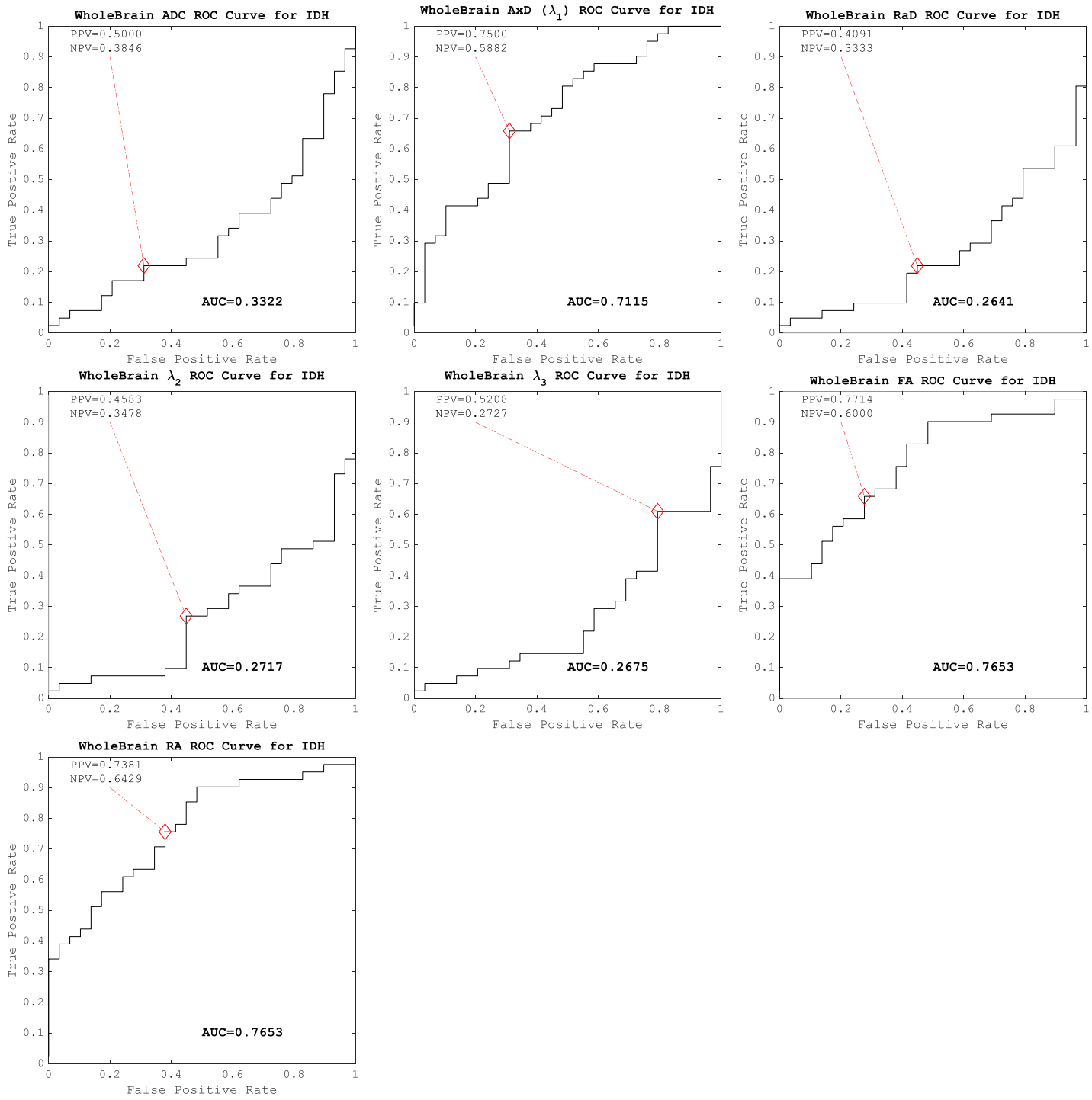

Figure S.1 ROC curves (Value>=Threshold) for IDH mutation from different indices from the whole brain showing area under the curve (AUC), optimal operating point (red diamond) and corresponding positive prediction value (PPV) and negative predictive value (NPV).

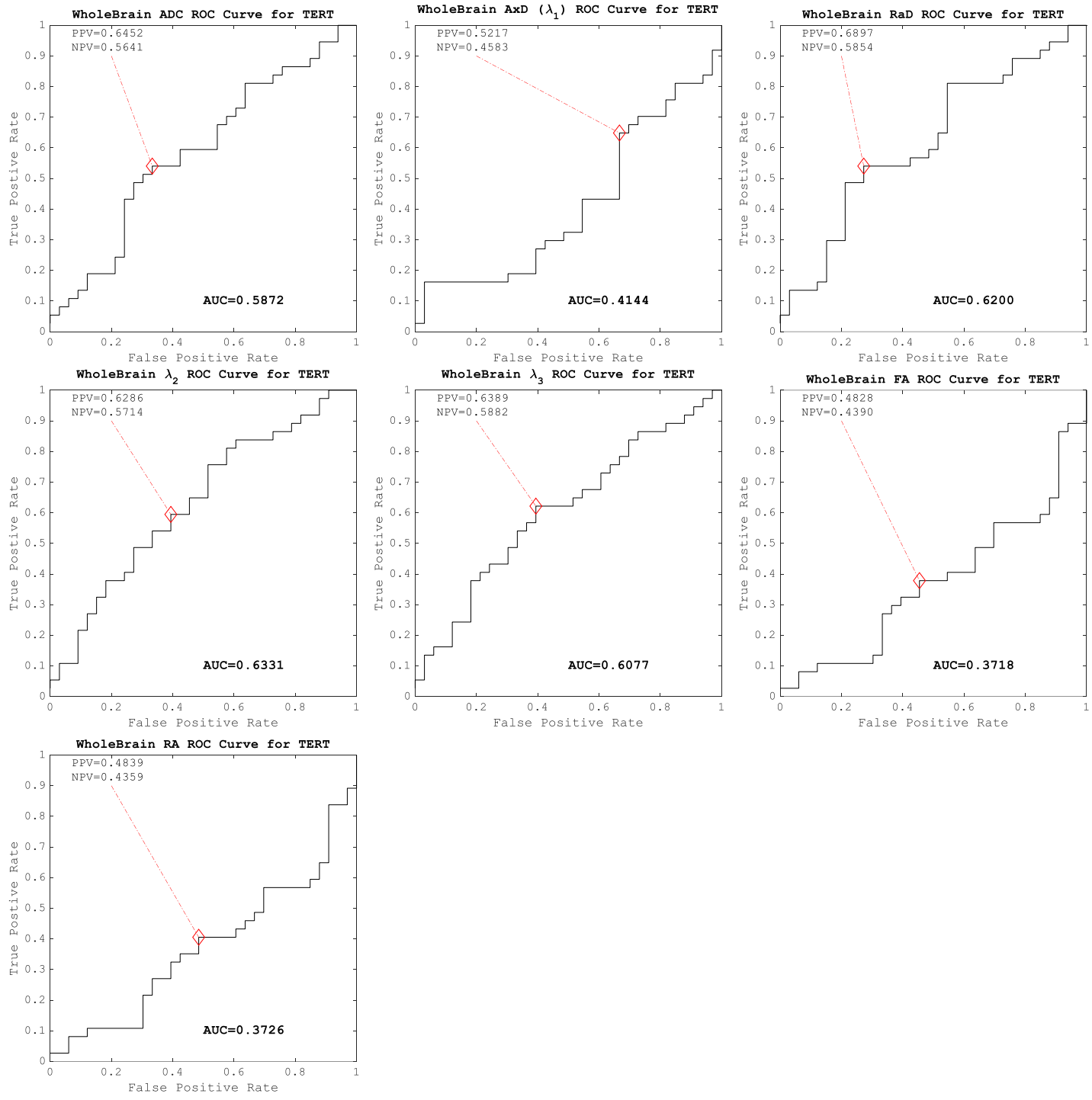

Figure S.2 ROC curves (Value>=Threshold) for TERT mutation from different indices from the whole brain showing area under the curve (AUC), optimal operating point (red diamond) and corresponding positive prediction value (PPV) and negative predictive value (NPV).

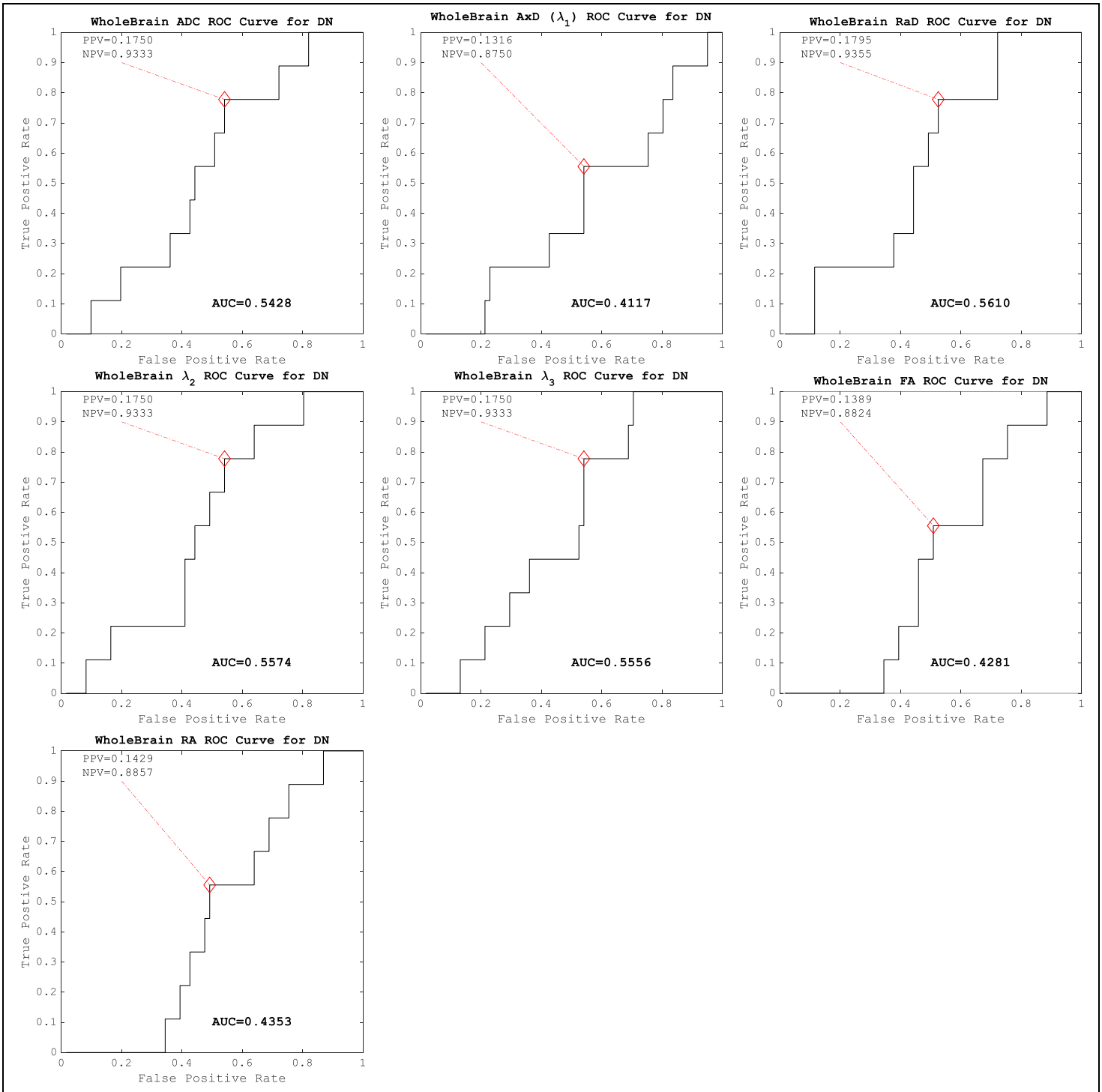

Figure S.3 ROC curves (Value>=Threshold) for Double Negative (DN) group from different indices from the whole brain showing area under the curve (AUC), optimal operating point (red diamond) and corresponding positive prediction value (PPV) and negative predictive value (NPV).

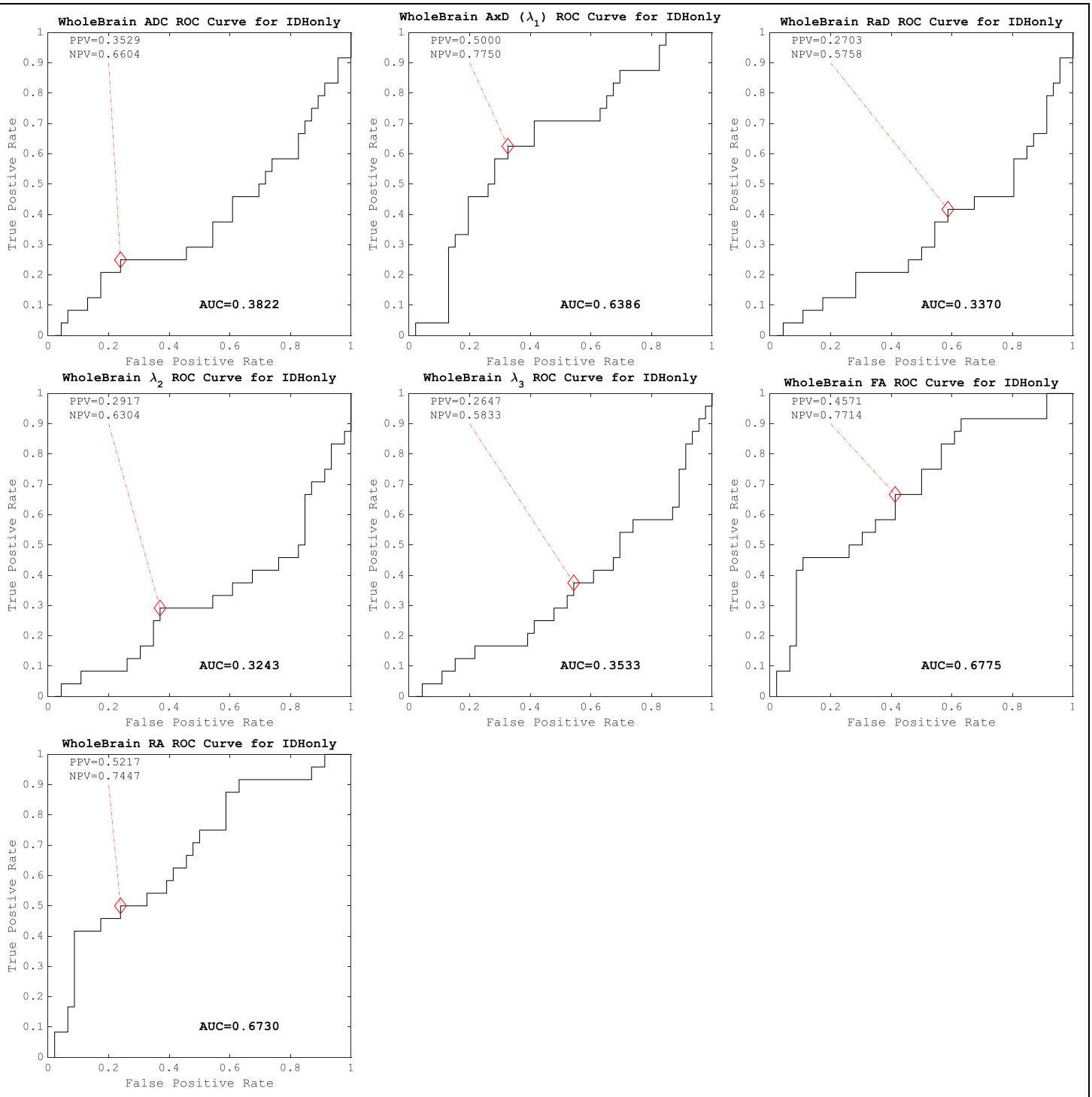

Figure S.4 ROC curves (Value>=Threshold) for IDHonly group from different indices from the whole brain showing area under the curve (AUC), optimal operating point (red diamond) and corresponding positive prediction value (PPV) and negative predictive value (NPV).

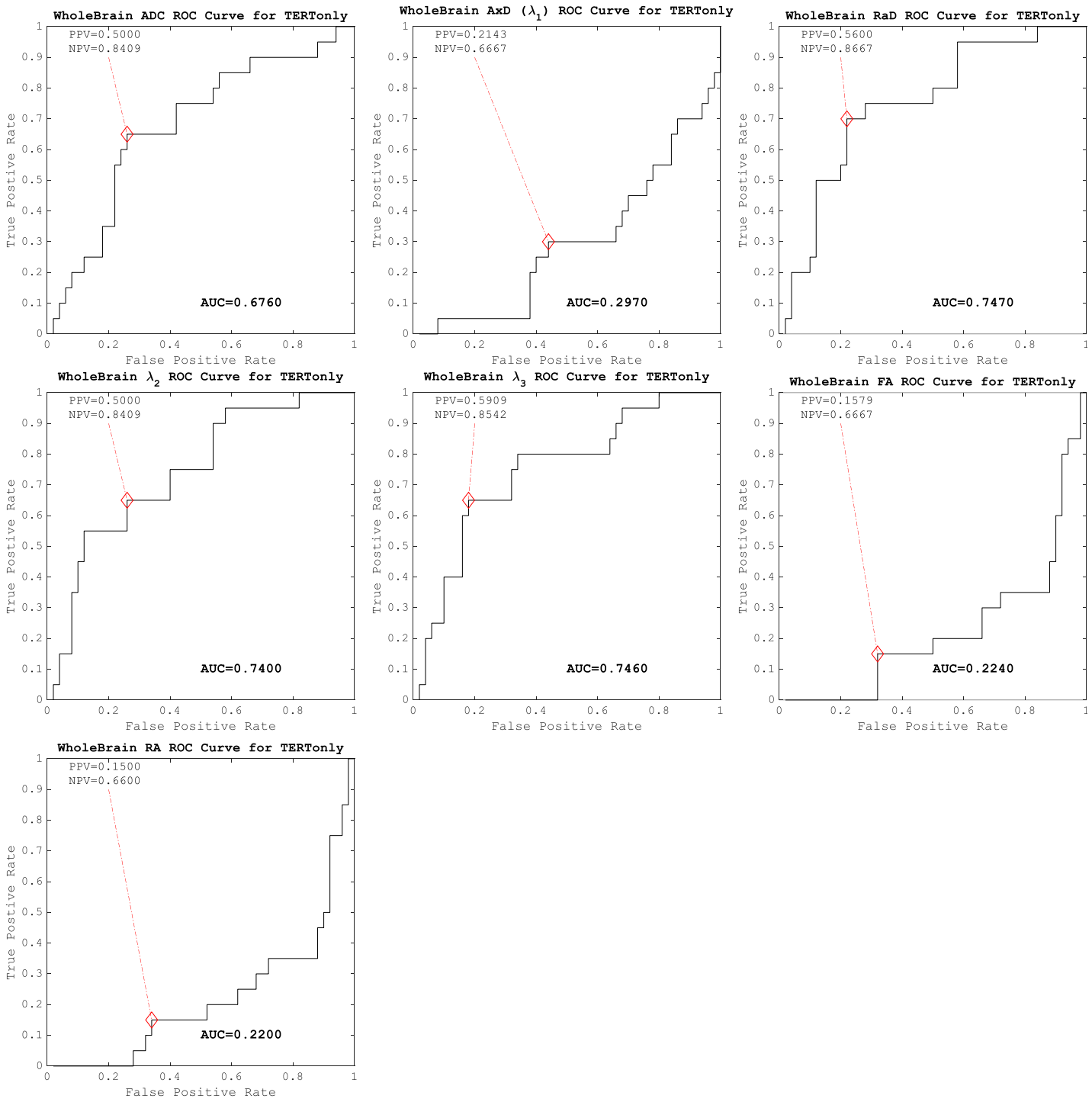

Figure S.5 ROC curves (Value>=Threshold) for TERTonly group from different indices from the whole brain showing area under the curve (AUC), optimal operating point (red diamond) and corresponding positive prediction value (PPV) and negative predictive value (NPV).

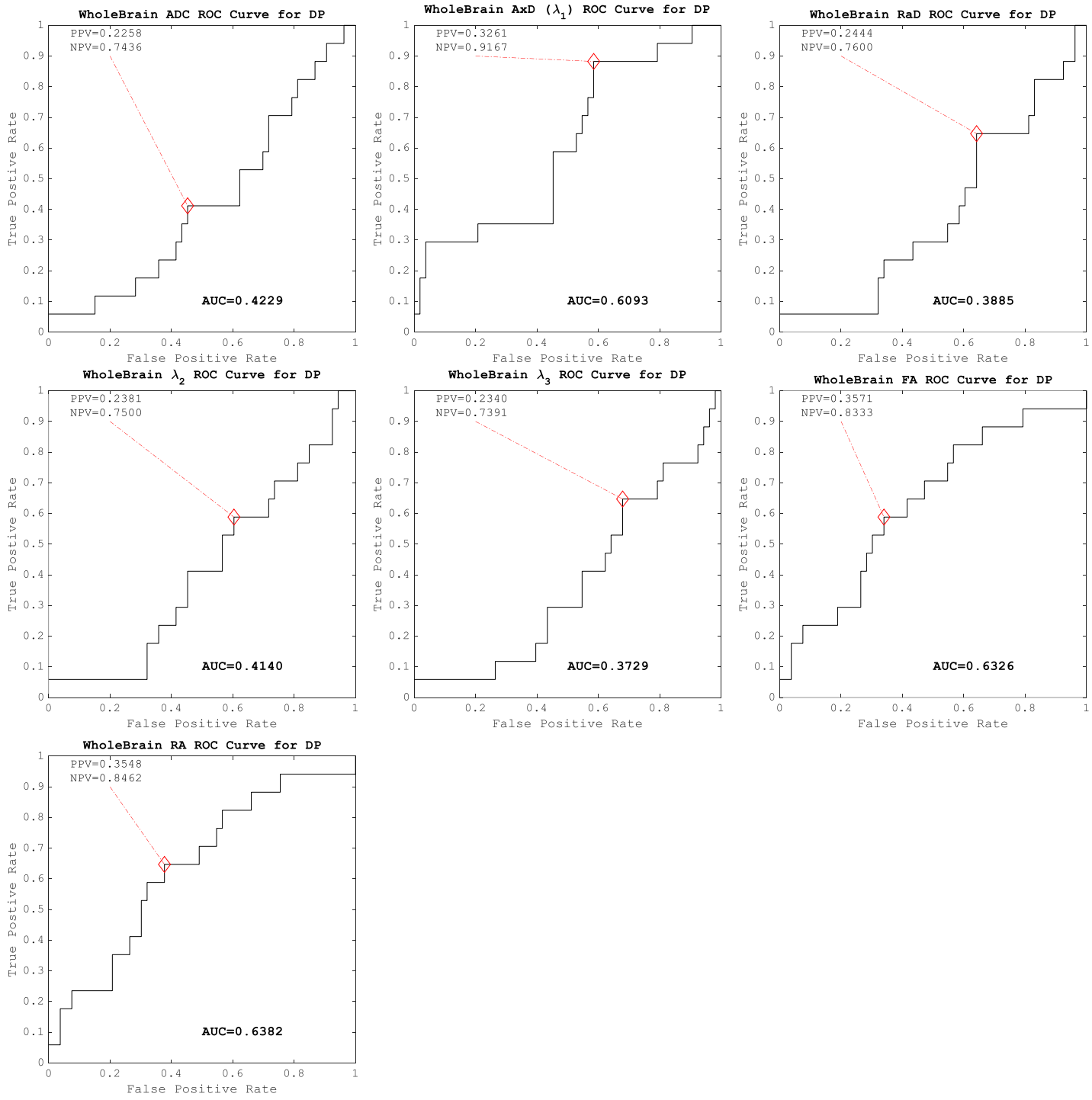

Figure S.6 ROC curves (Value>=Threshold) for double positive (DP) group from different indices from the whole brain showing area under the curve (AUC), optimal operating point (red diamond) and corresponding positive prediction value (PPV) and negative predictive value (NPV).

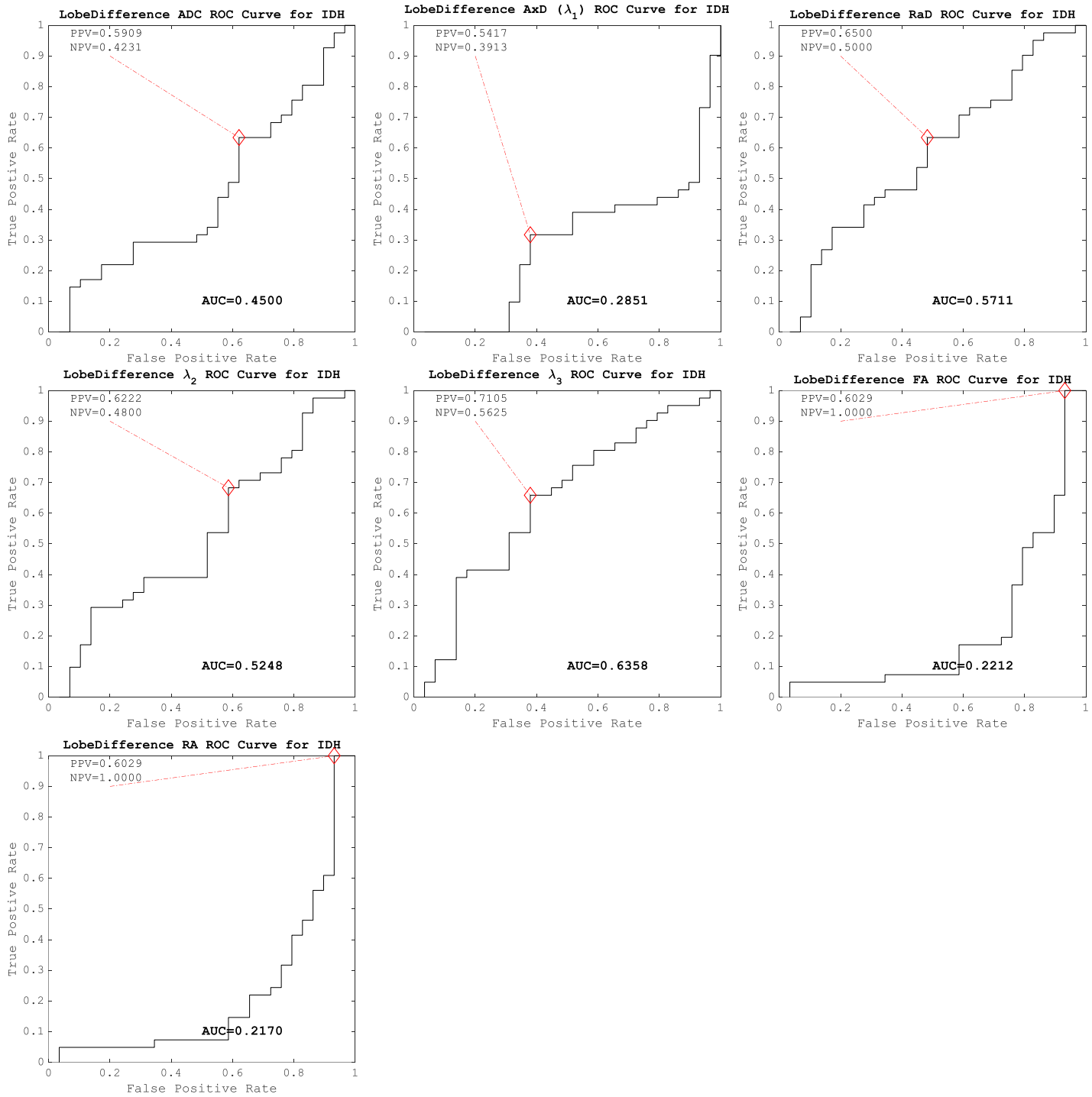

Figure S.7 ROC curves (Value>=Threshold) for IDH mutation from different indices from the hemispheric differences showing area under the curve (AUC), optimal operating point (red diamond) and corresponding positive prediction value (PPV) and negative predictive value (NPV).

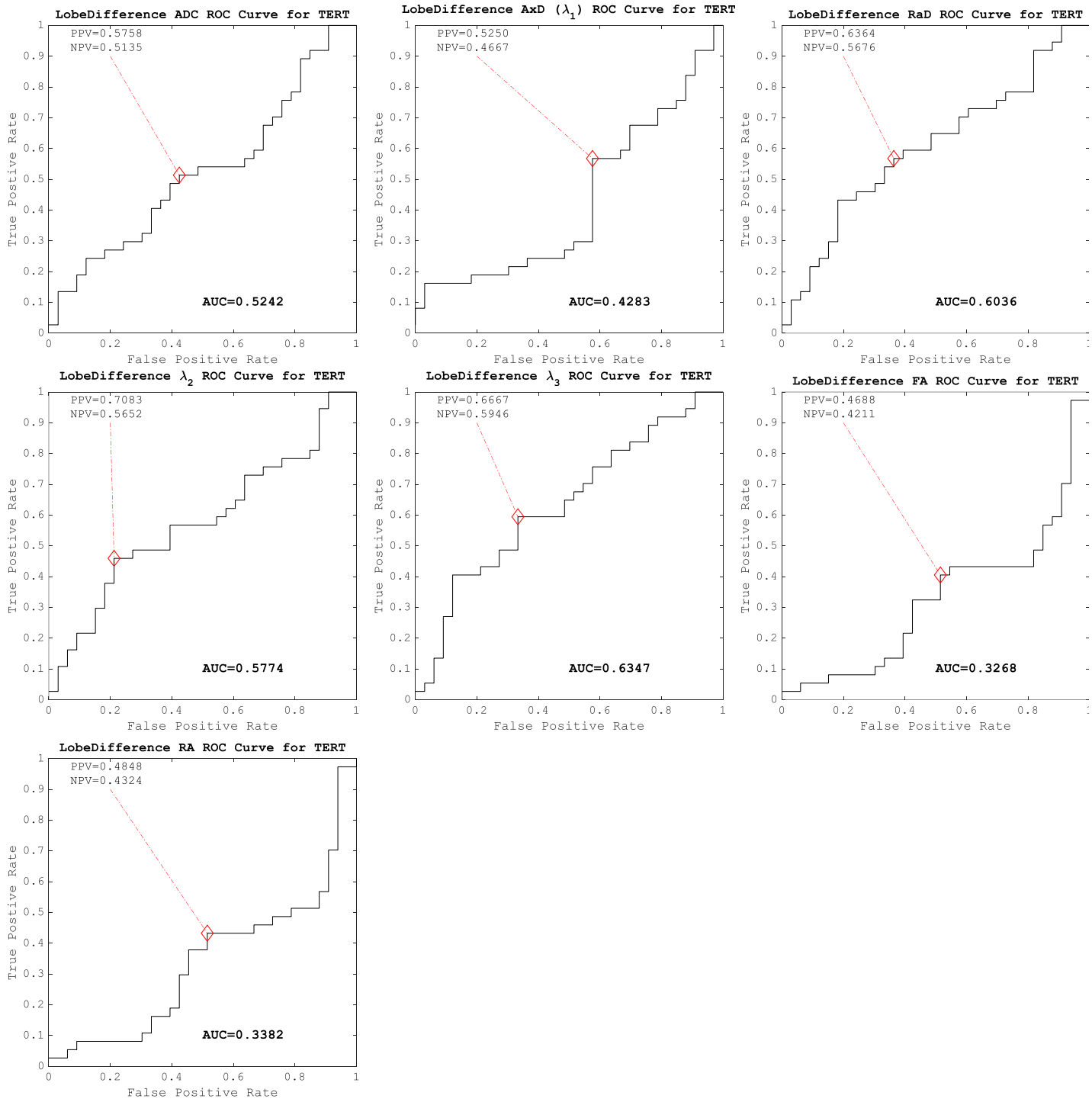

Figure S.8 ROC curves (Value>=Threshold) for TERT mutation from different indices from the hemispheric differences showing area under the curve (AUC), optimal operating point (red diamond) and corresponding positive prediction value (PPV) and negative predictive value (NPV).

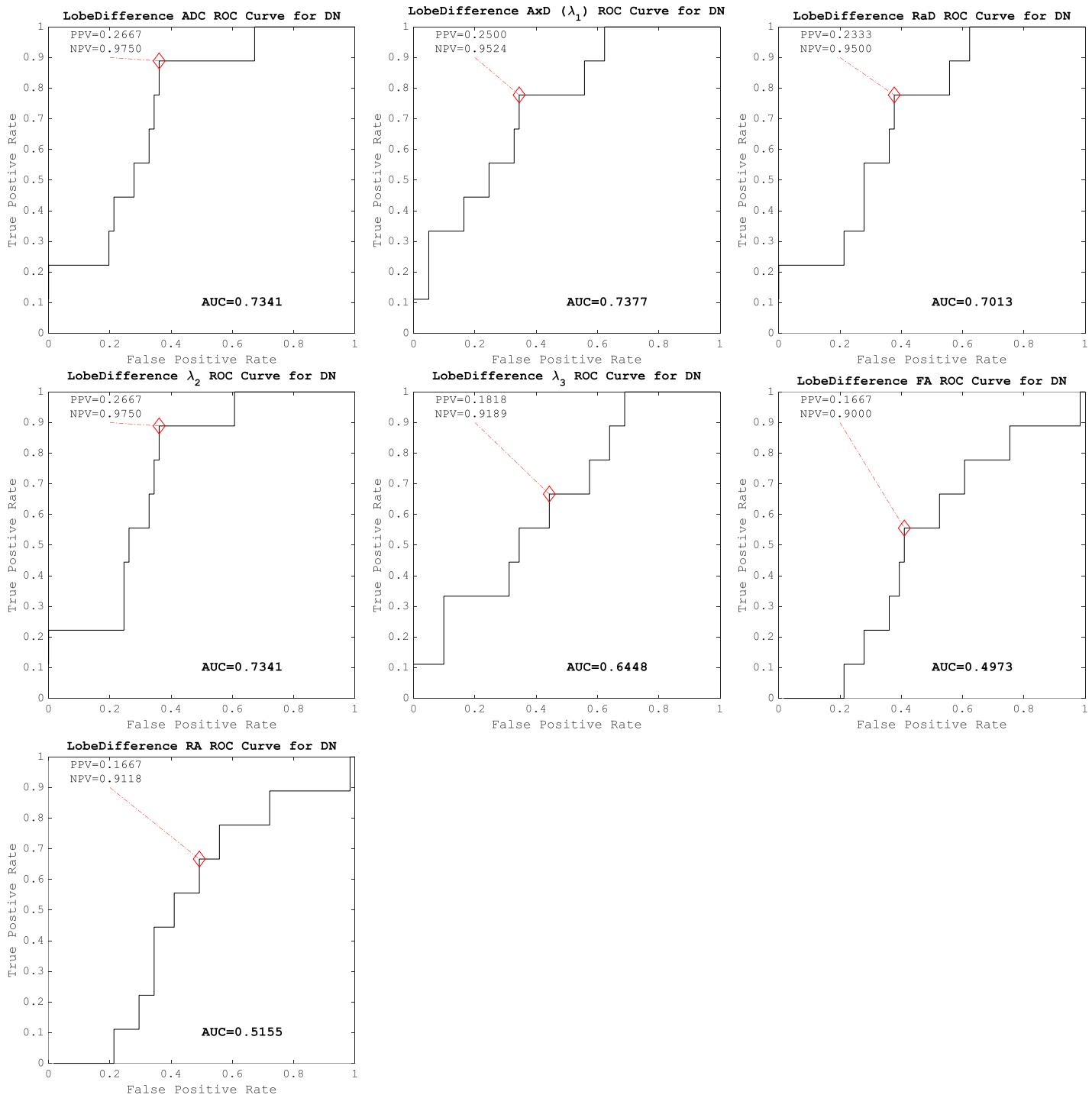

Figure S.9 ROC curves (Value>=Threshold) for Double Negative (DN) group from different indices from the hemispheric differences showing area under the curve (AUC), optimal operating point (red diamond) and corresponding positive prediction value (PPV) and negative predictive value (NPV).

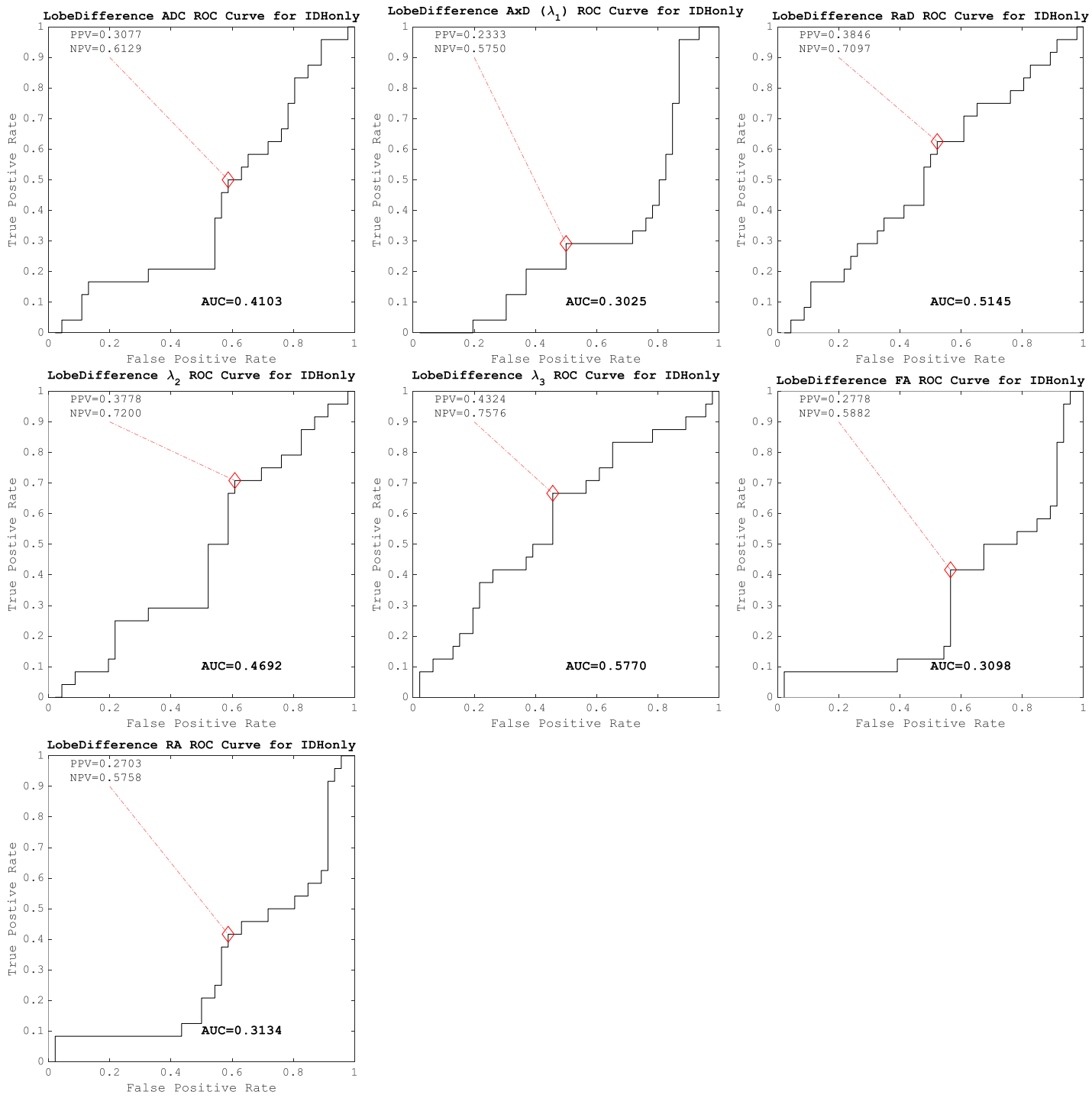

Figure S.10 ROC curves (Value>=Threshold) for IDHonly group from different indices from the hemispheric differences showing area under the curve (AUC), optimal operating point (red diamond) and corresponding positive prediction value (PPV) and negative predictive value (NPV).

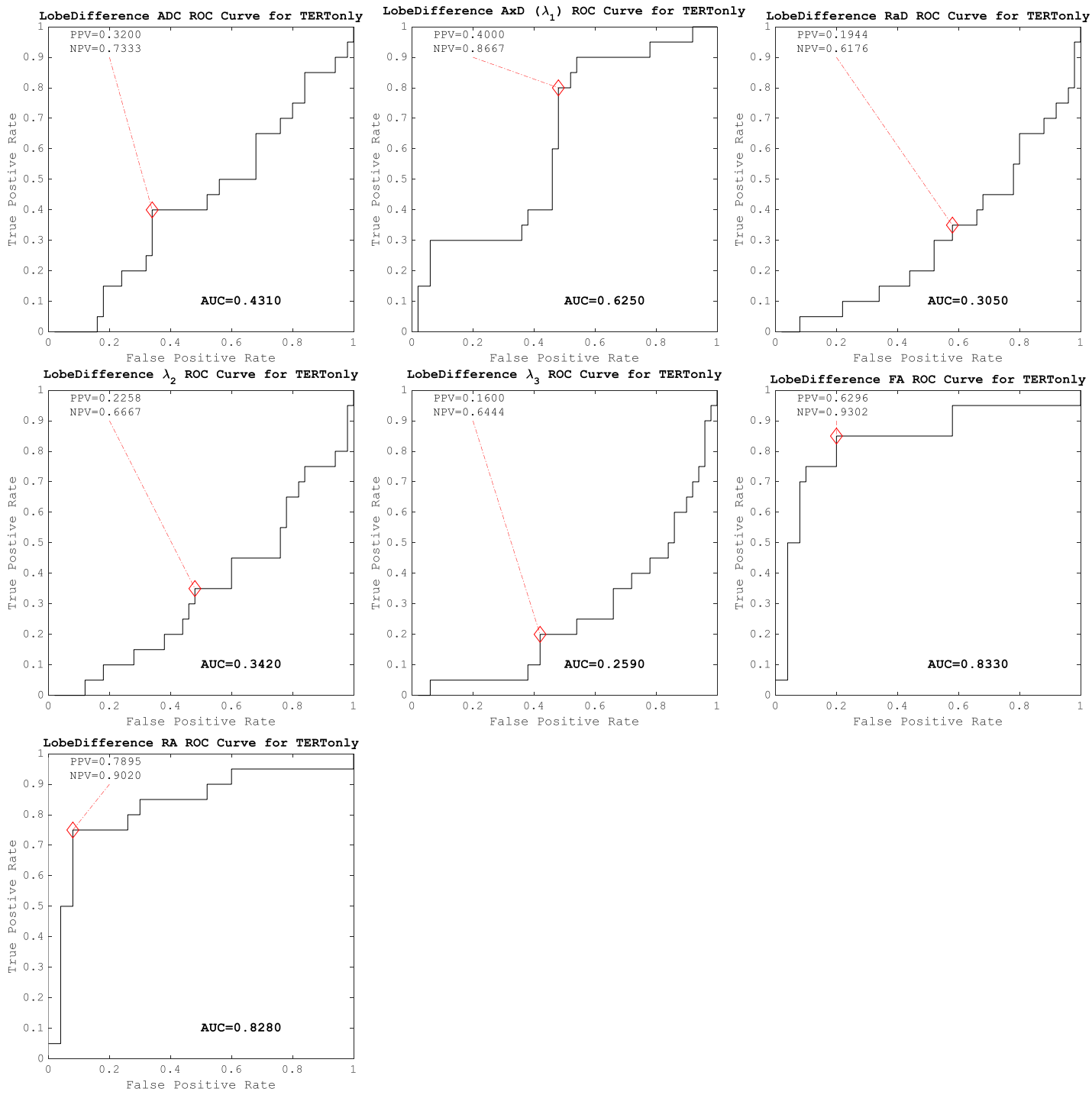

Figure S.11 ROC curves (Value>=Threshold) for TERTonly group from different indices from the hemispheric differences showing area under the curve (AUC), optimal operating point (red diamond) and corresponding positive prediction value (PPV) and negative predictive value (NPV).

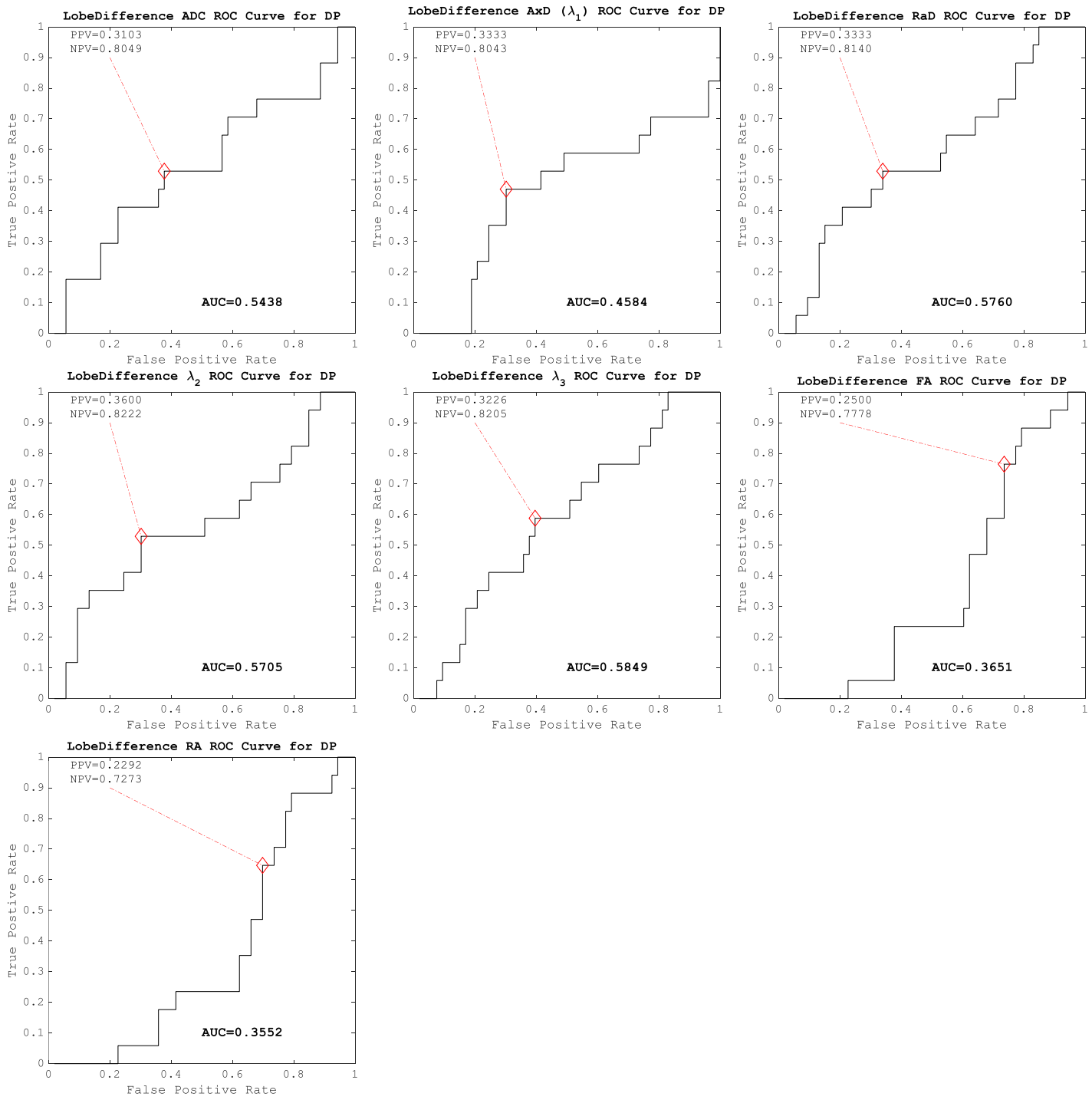

Figure S.12 ROC curves (Value>=Threshold) for double positive (DP) group from different indices from the hemispheric differences showing area under the curve (AUC), optimal operating point (red diamond) and corresponding positive prediction value (PPV) and negative predictive value (NPV).

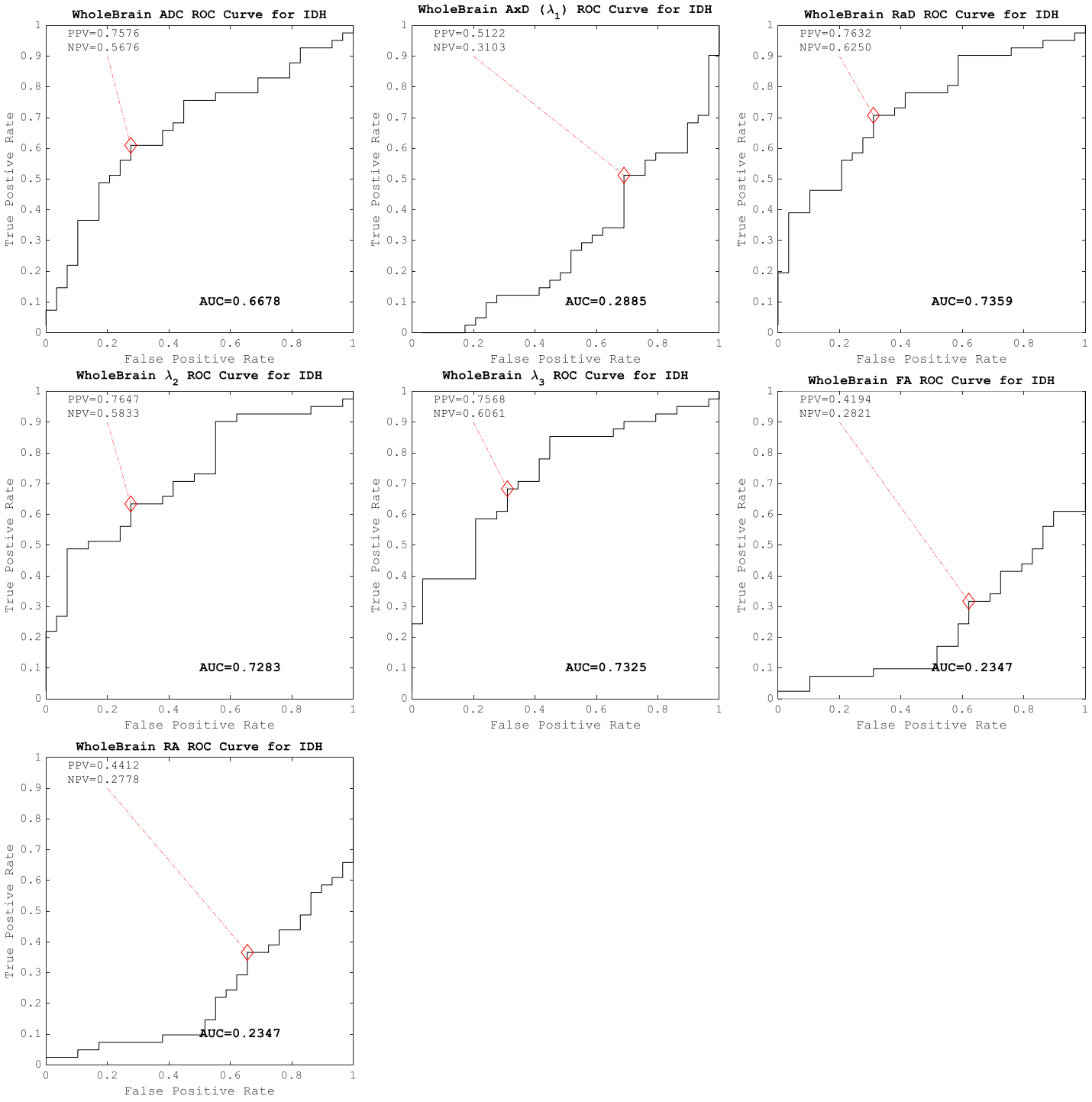

Figure S.13 ROC curves (Value<=Threshold) for IDH mutation from different indices from the whole brain showing area under the curve (AUC), optimal operating point (red diamond) and corresponding positive prediction value (PPV) and negative predictive value (NPV).

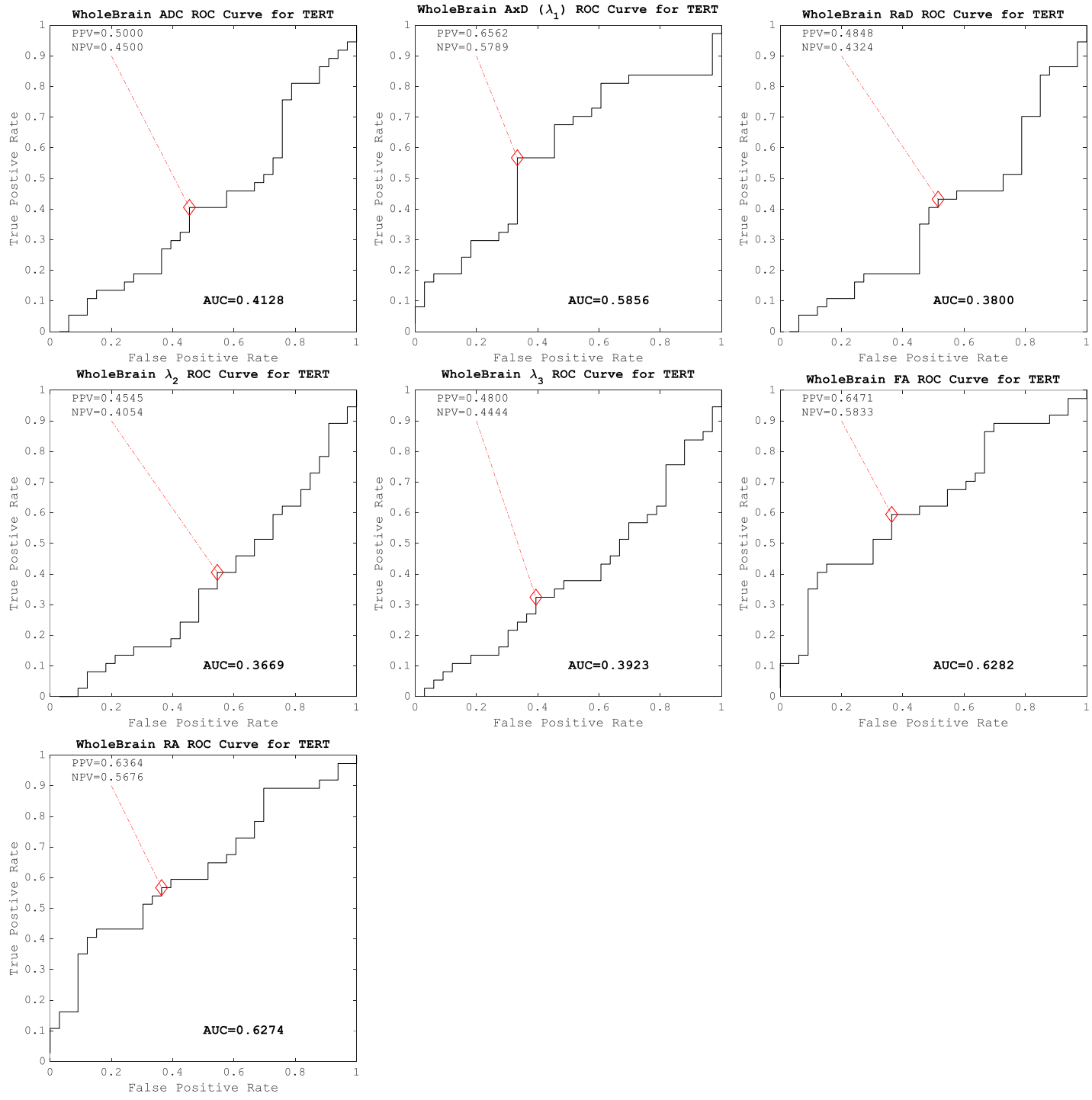

Figure S.14 ROC curves (Value<=Threshold) for TERT mutation from different indices from the whole brain showing area under the curve (AUC), optimal operating point (red diamond) and corresponding positive prediction value (PPV) and negative predictive value (NPV).

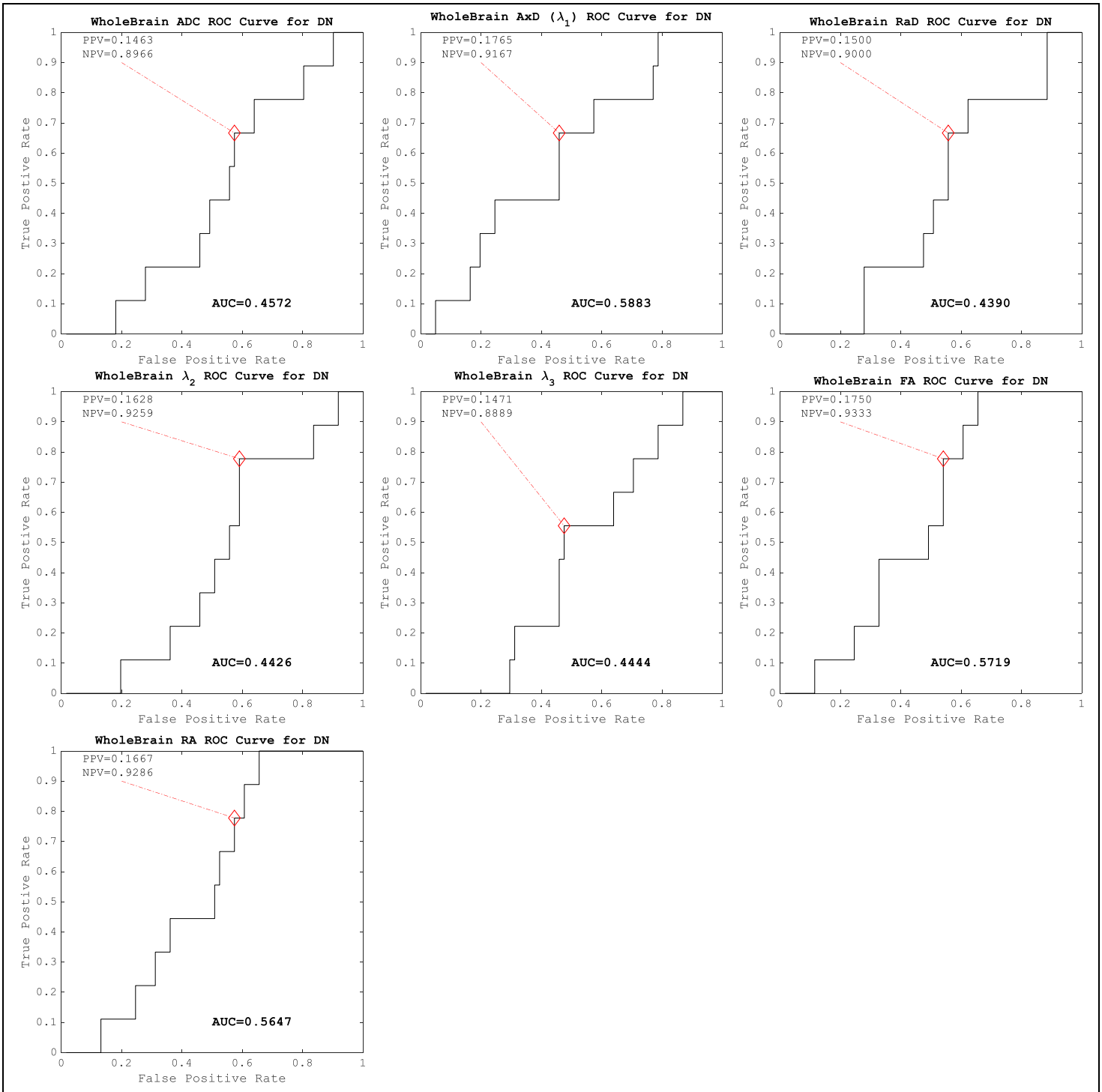

Figure S.15 ROC curves (Value<=Threshold) for Double Negative (DN) group from different indices from the whole brain showing area under the curve (AUC), optimal operating point (red diamond) and corresponding positive prediction value (PPV) and negative predictive value (NPV).

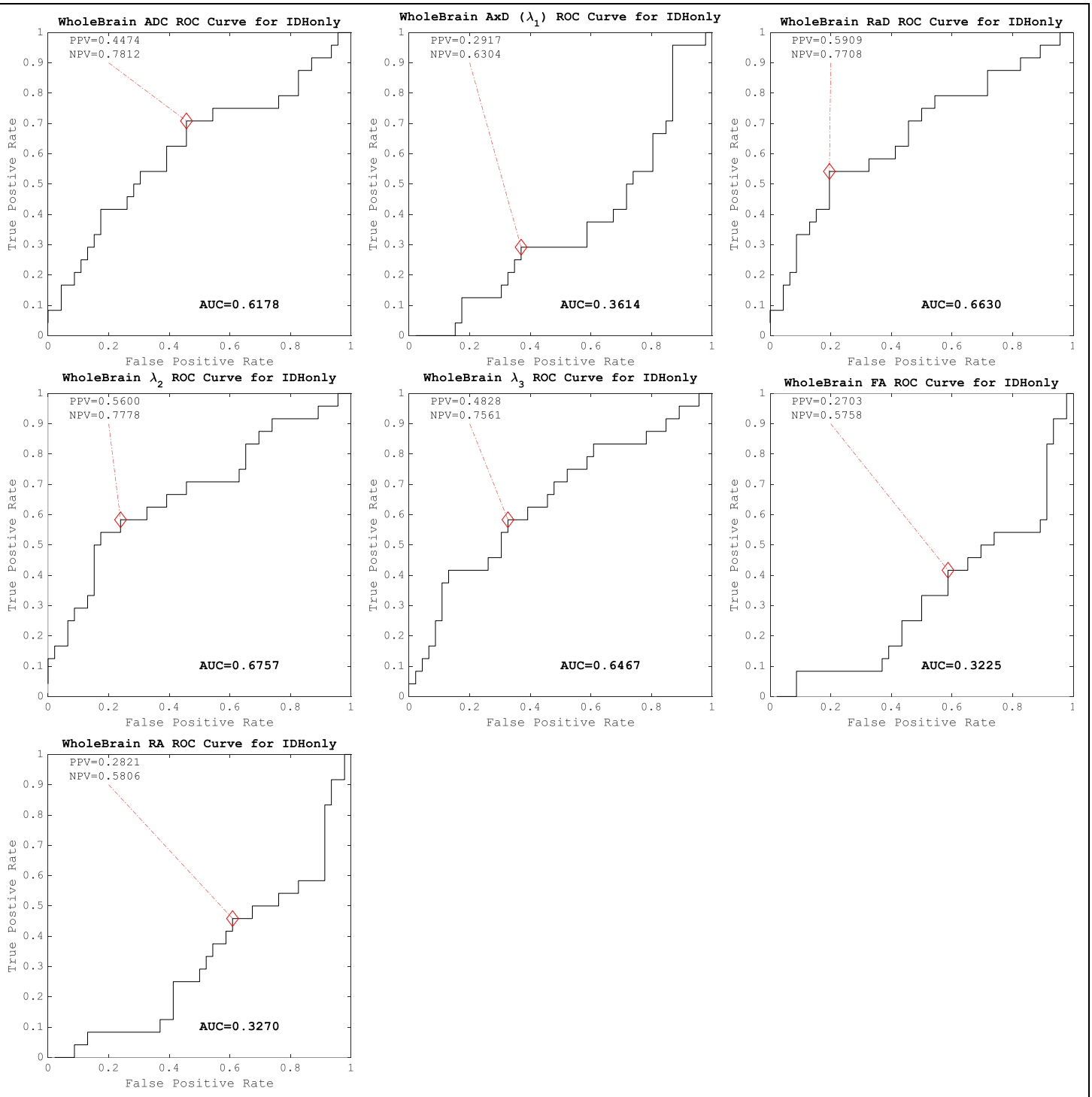

Figure S.16 ROC curves (Value<=Threshold) for IDHonly group from different indices from the whole brain showing area under the curve (AUC), optimal operating point (red diamond) and corresponding positive prediction value (PPV) and negative predictive value (NPV).

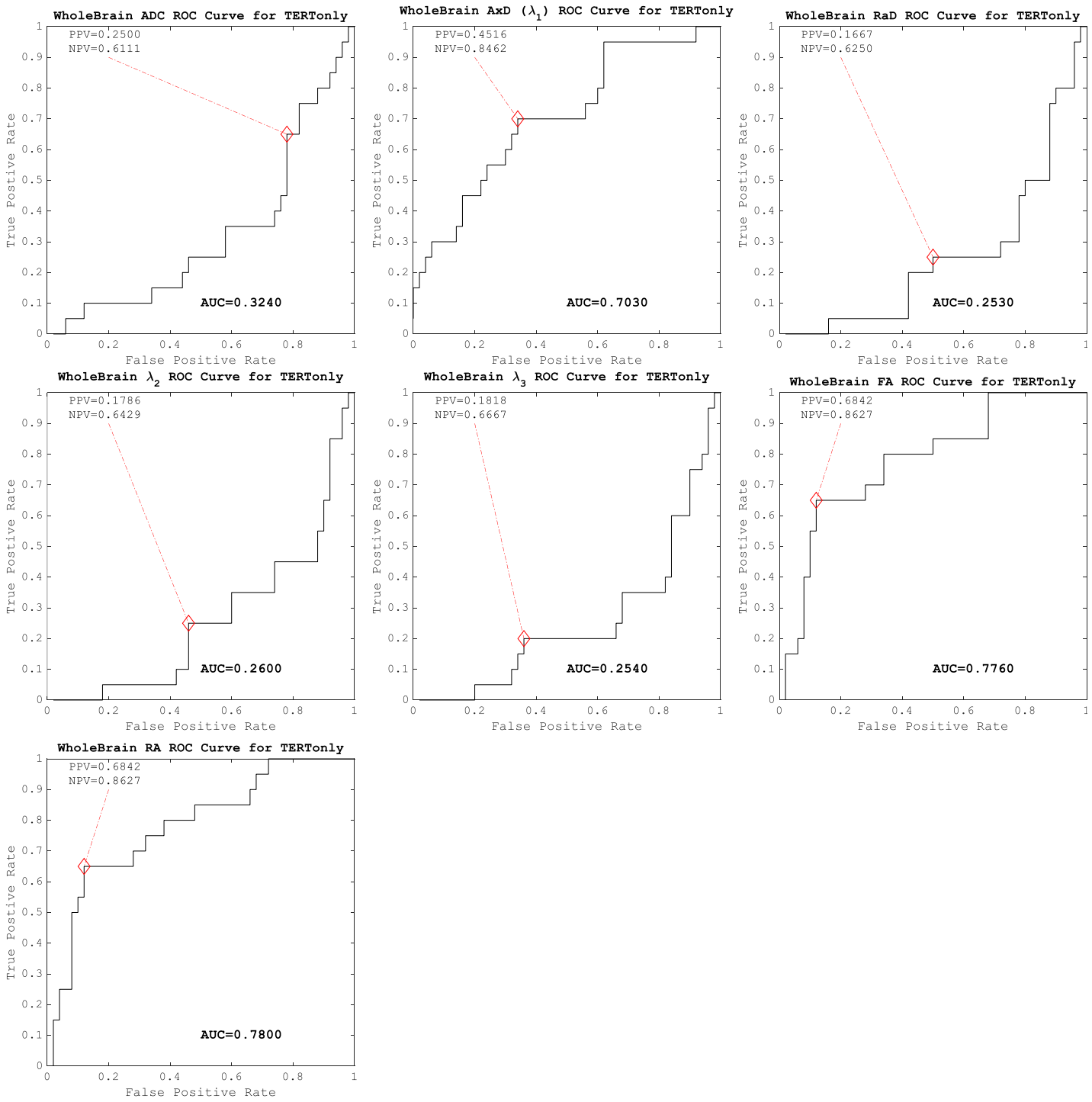

Figure S.17 ROC curves (Value<=Threshold) for TERTonly group from different indices from the whole brain showing area under the curve (AUC), optimal operating point (red diamond) and corresponding positive prediction value (PPV) and negative predictive value (NPV).

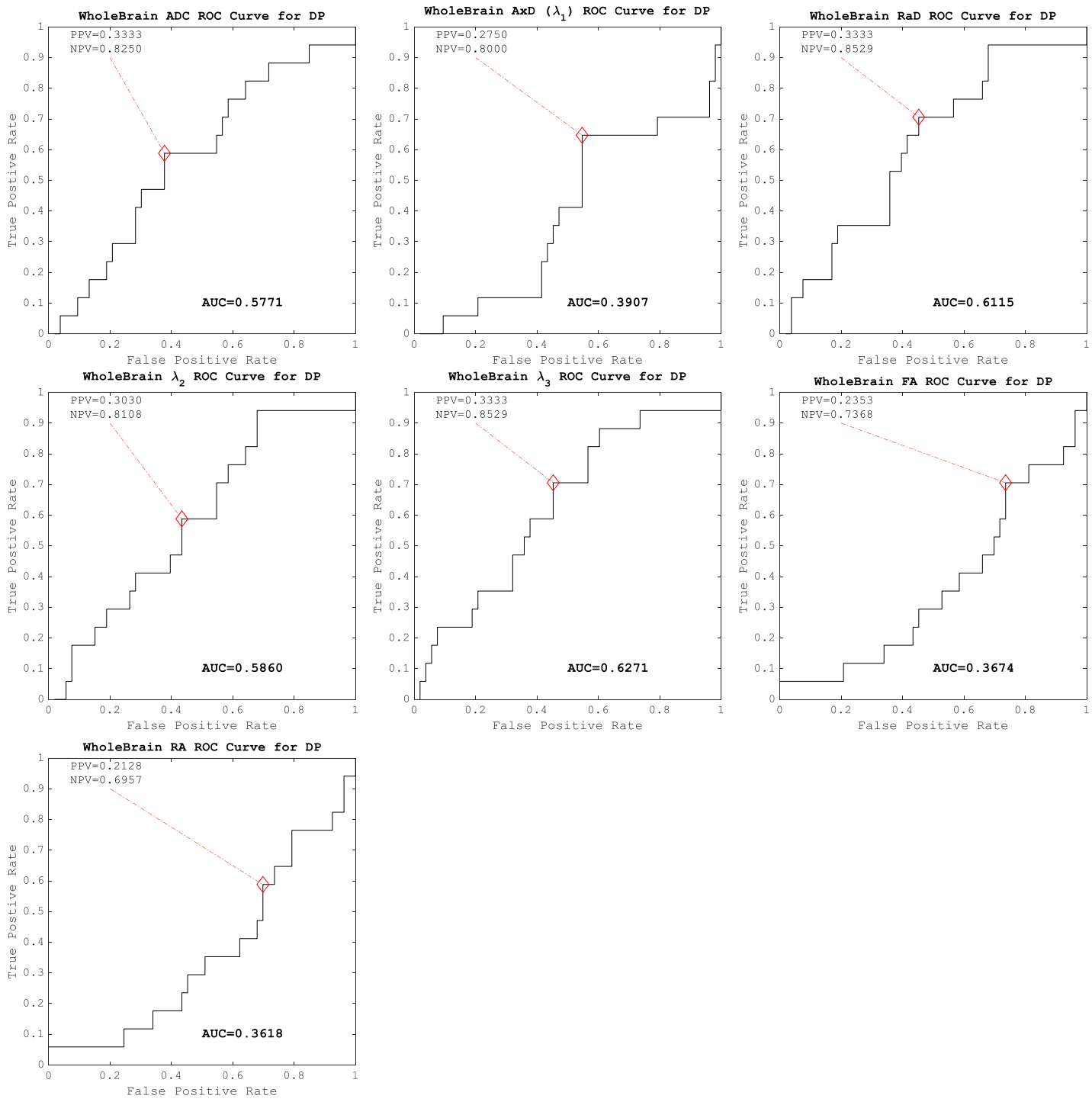

Figure S.18 ROC curves (Value<=Threshold) for double positive (DP) group from different indices from the whole brain showing area under the curve (AUC), optimal operating point (red diamond) and corresponding positive prediction value (PPV) and negative predictive value (NPV).

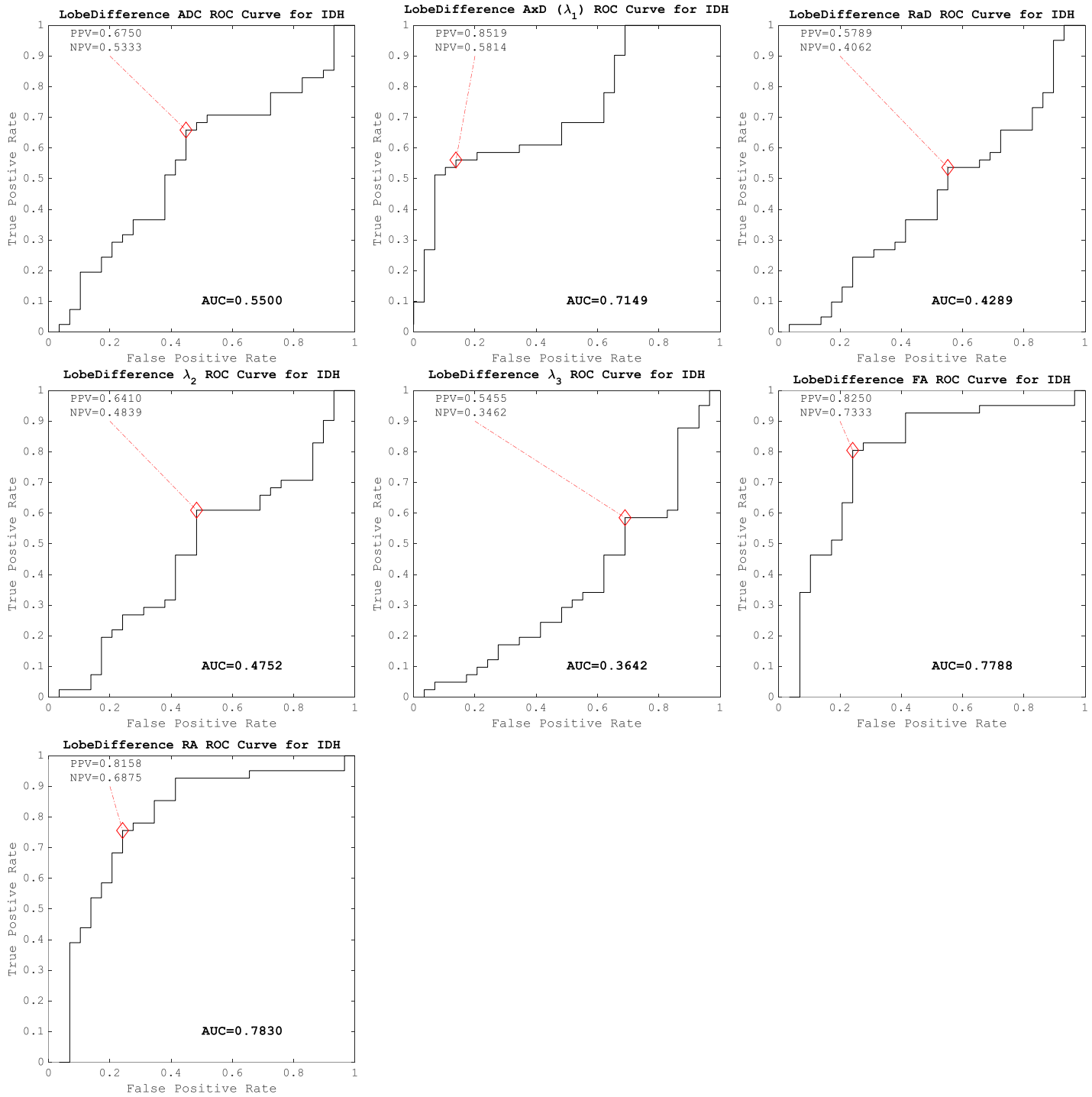

Figure S.19 ROC curves (Value<=Threshold) for IDH mutation from different indices from the hemispheric differences showing area under the curve (AUC), optimal operating point (red diamond) and corresponding positive prediction value (PPV) and negative predictive value (NPV).

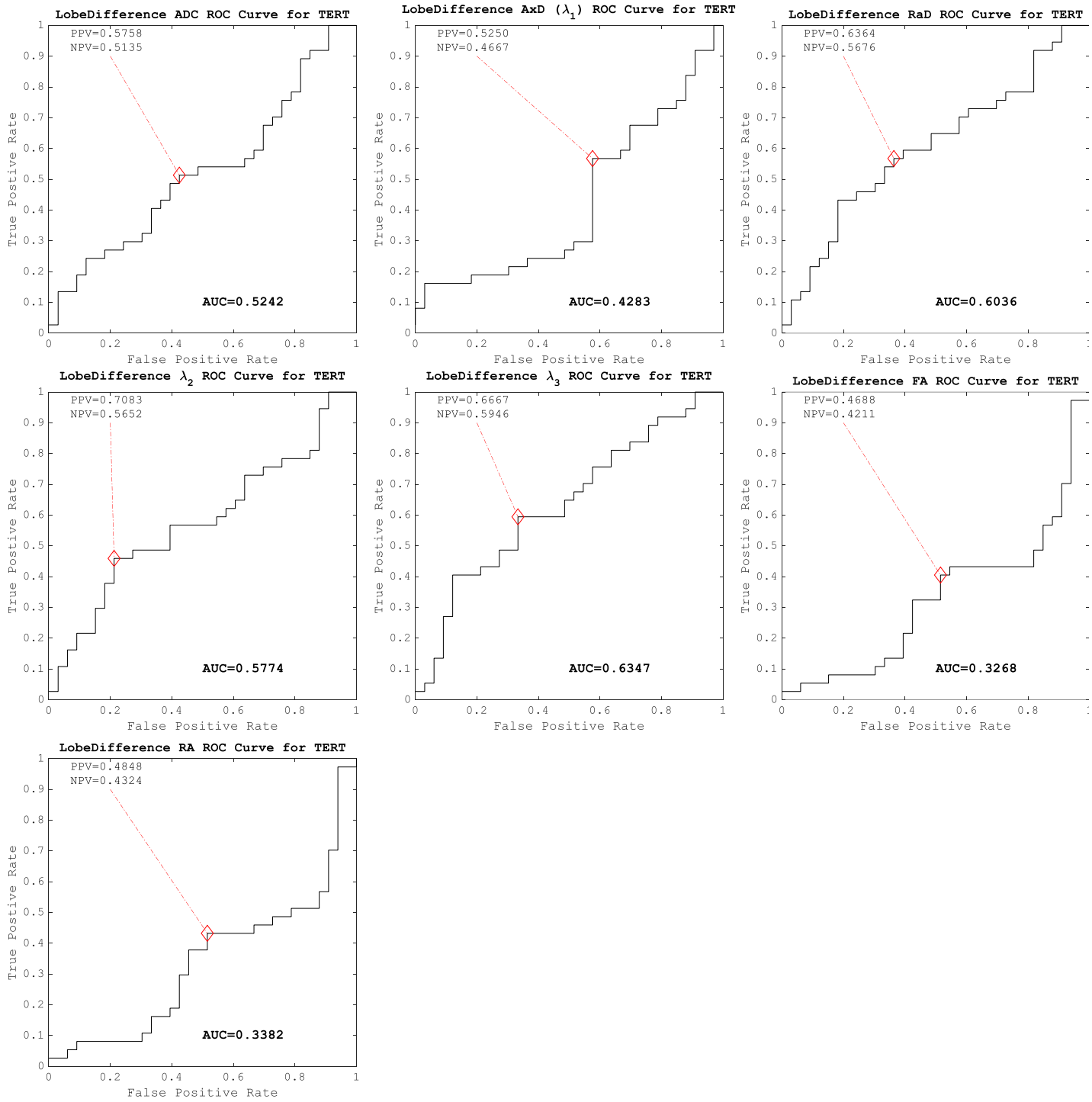

Figure S.20 ROC curves (Value<=Threshold) for TERT mutation from different indices from the hemispheric differences showing area under the curve (AUC), optimal operating point (red diamond) and corresponding positive prediction value (PPV) and negative predictive value (NPV).

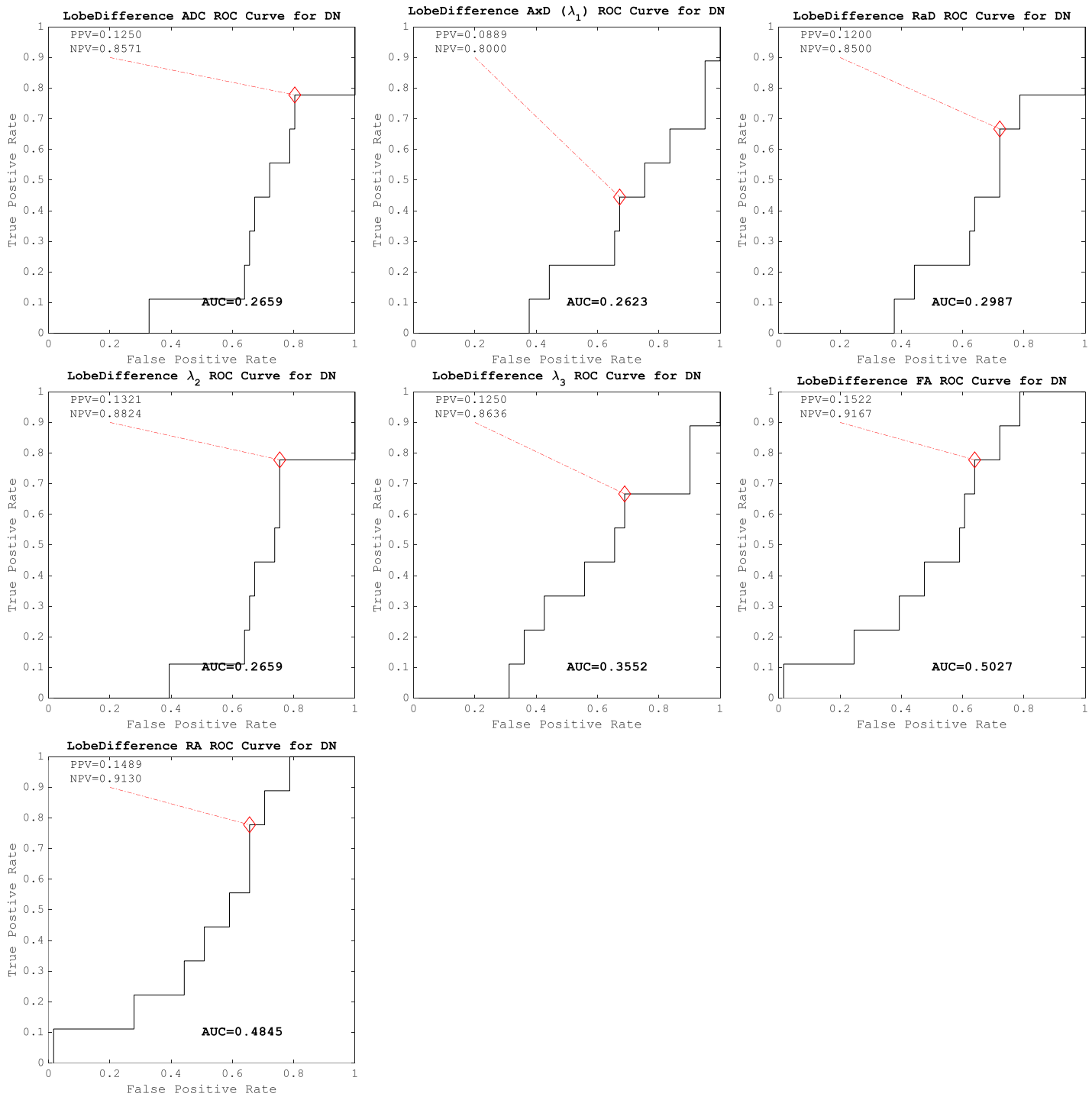

Figure S.21 ROC curves (Value<=Threshold) for Double Negative (DN) group from different indices from the hemispheric differences showing area under the curve (AUC), optimal operating point (red diamond) and corresponding positive prediction value (PPV) and negative predictive value (NPV).

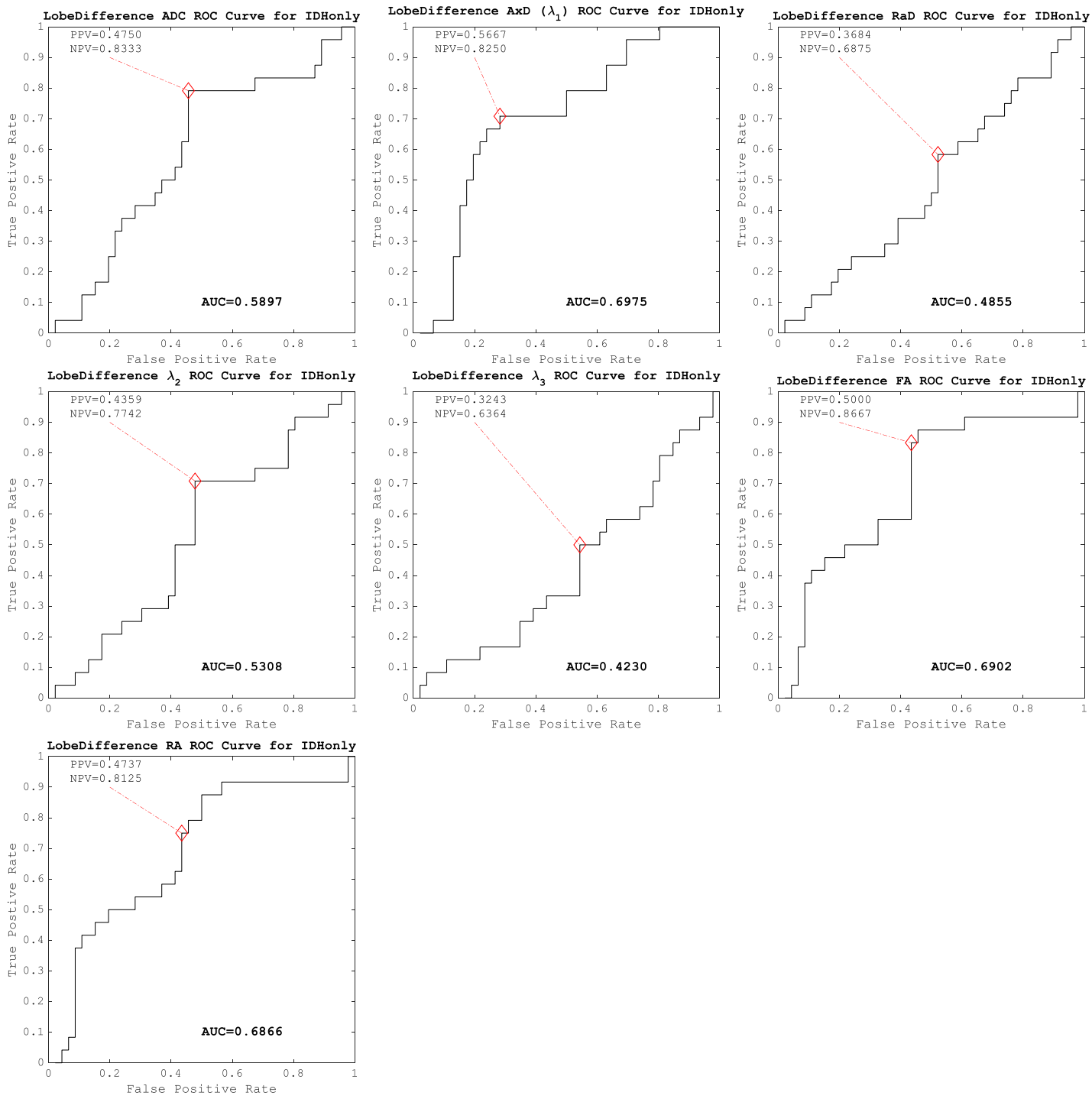

Figure S.22 ROC curves (Value<=Threshold) for IDHonly group from different indices from the hemispheric differences showing area under the curve (AUC), optimal operating point (red diamond) and corresponding positive prediction value (PPV) and negative predictive value (NPV).

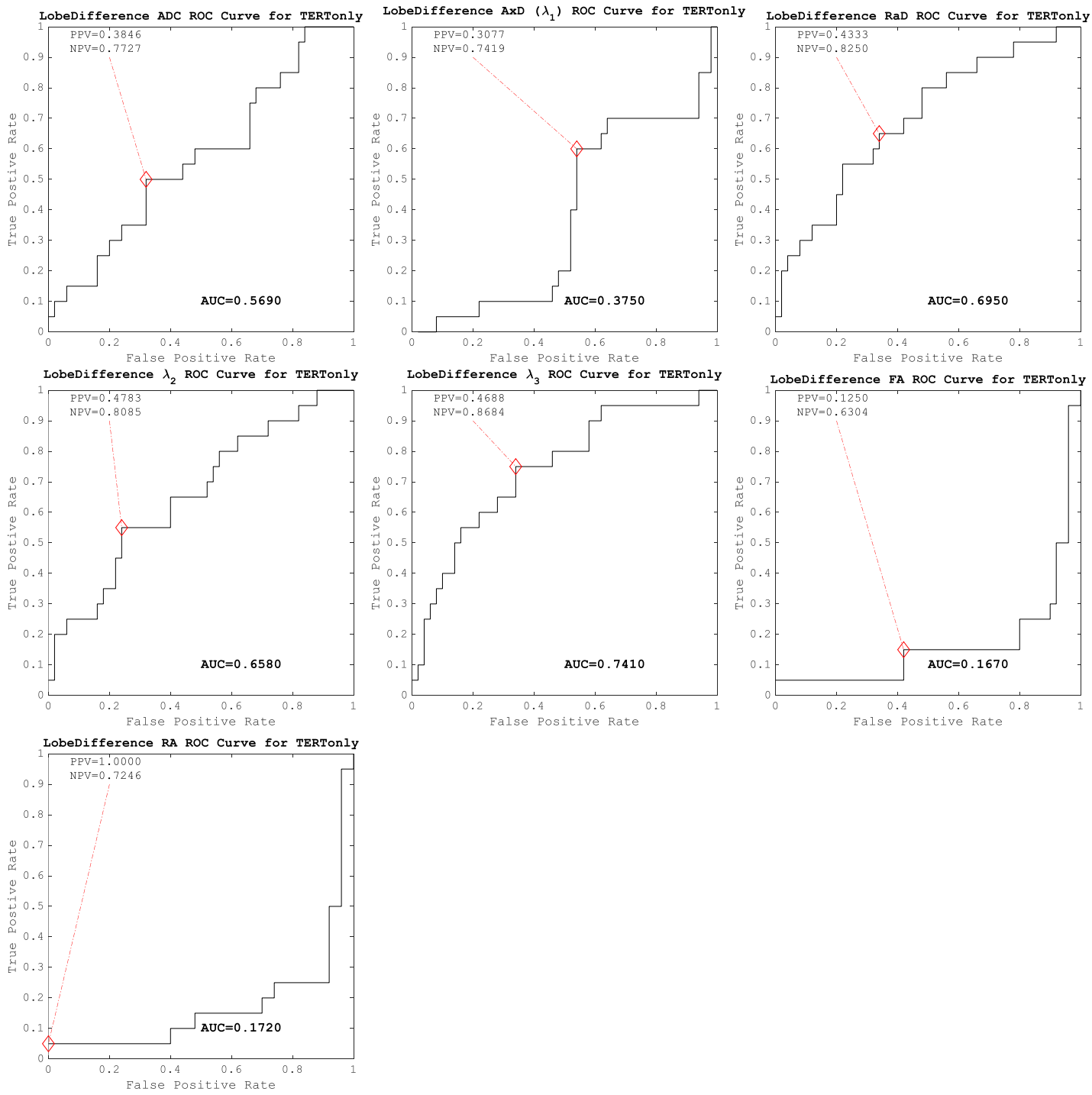

Figure S.23 ROC curves (Value<=Threshold) for TERTonly group from different indices from the hemispheric differences showing area under the curve (AUC), optimal operating point (red diamond) and corresponding positive prediction value (PPV) and negative predictive value (NPV).

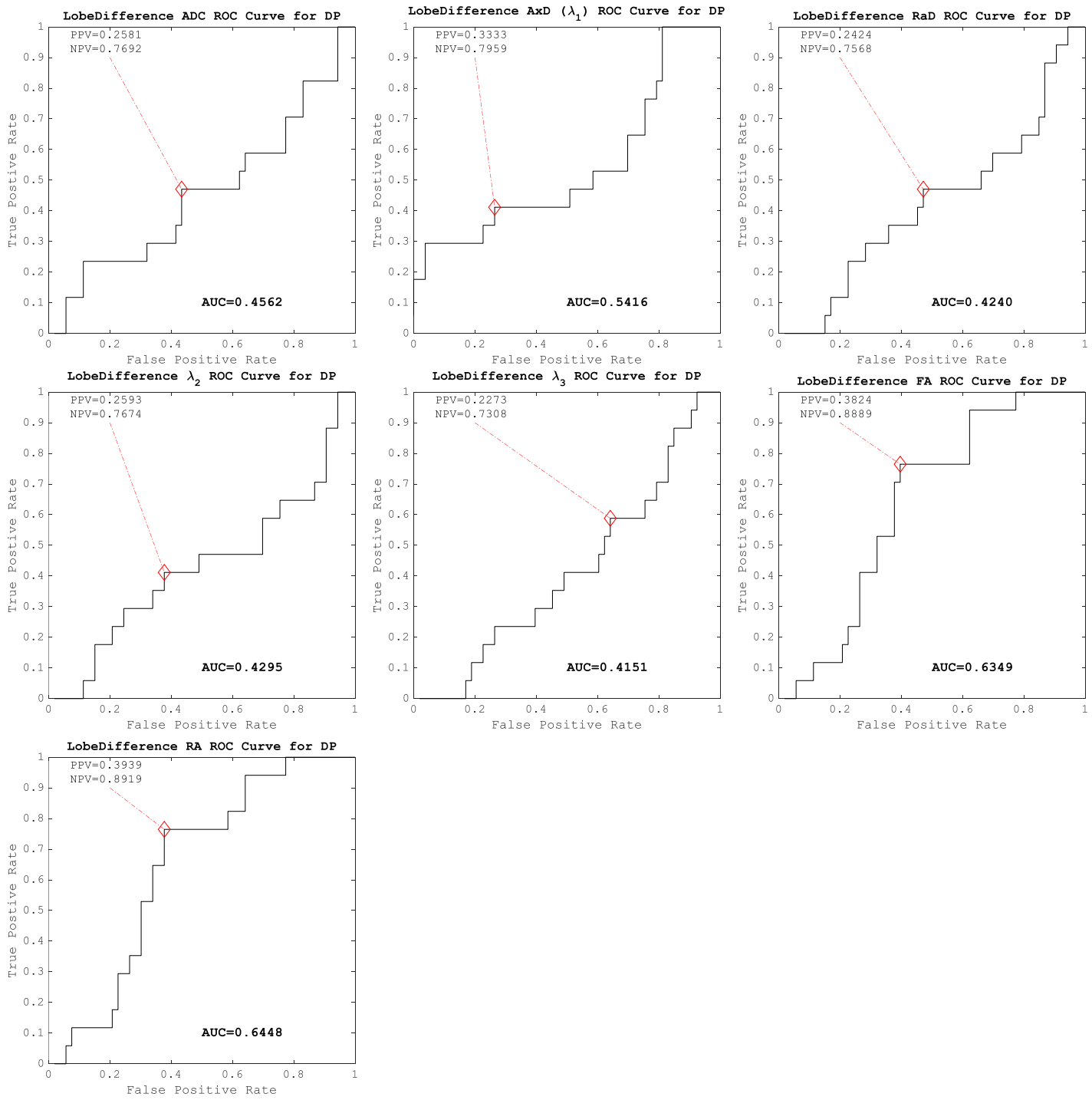

Figure S.24 ROC curves (Value<=Threshold) for double positive (DP) group from different indices from the hemispheric differences showing area under the curve (AUC), optimal operating point (red diamond) and corresponding positive prediction value (PPV) and negative predictive value (NPV).

SUPPLEMENTAL REFERENCES

1. Basser PJ, Pierpaoli C. Microstructural and Physiological Features of Tissues Elucidated by Quantitative-Diffusion-Tensor MRI. *Journal of Magnetic Resonance, Series B.* 1996; 111(3):209-219.

2. Song S-K, Sun S-W, Ramsbottom MJ, Chang C, Russell J, Cross AH. Dysmyelination Revealed through MRI as Increased Radial (but Unchanged Axial) Diffusion of Water. *Neuroimage.* 2002; 17(3):1429-1436.

3. Glantz S. *Primer of Biostatistics*. 7 ed: McGraw Hill; 2011.

4. Pearson ES, Hartley HO. Charts of The Power Function for Analysis of Variance Tests, Derived From The Non-Central F-Distribution. *Biometrika.* 1951; 38(1-2):112-130.

5. Rosner B. *Fundamentals of Biostatistics*. 8th edition. ed. Boston, MA: Cengage Learning; 2016.

6. Fawcett T. An introduction to ROC analysis. *Pattern Recognition Letters.* 2006; 27(8):861-874.